The thermal structure of subduction zone back arcs

Claire A. Currie[1,2] and Roy D. Hyndman[1,3]

Received 2 September 2005; revised 21 April 2006; accepted 4 May 2006; published 17 August 2006.

[1] It is well recognized that active arc volcanism at nearly all subduction zones requires temperatures greater than 1200°C in the subarc mantle, despite the underthrusting cool subducting plate. In this study, we document evidence that high upper mantle temperatures are not restricted to the arc but usually extend for several hundred kilometers across the back arc, even in areas that have not undergone extension. For 10 circum-Pacific back arcs where there has been no significant recent extension, we have compiled observational constraints on the thermal structure using a number of independent indicators of mantle temperature, including surface heat flow, seismic velocity, and xenolith thermobarometry. The observations indicate uniformly high temperatures in the shallow mantle and a thin lithosphere (1200°C at ~60 km depth) over back-arc widths of 250 to >900 km. Similar high temperatures are inferred for extensional back arcs of the western Pacific and southern Europe, but the thermal structures are complicated by extension and spreading. A broad hot back arc may be a fundamental characteristic of a subduction zone that places important constraints on back-arc mantle dynamics. In particular, the thermal structure predicted for slab-driven corner flow is inconsistent with the observed uniformly high back-arc temperatures. We favor the alternate model that heat is rapidly carried upward from depth by vigorous thermal convection in the back-arc upper mantle. Such convection may be promoted by low viscosities, resulting from hydration by fluids from the subducting plate. Following subduction termination, we find that the high temperatures decay over a timescale of about 300 Myr.

Citation: Currie, C. A., and R. D. Hyndman (2006), The thermal structure of subduction zone back arcs, *J. Geophys. Res.*, *111*, B08404, doi:10.1029/2005JB004024.

1. Introduction

[2] At subduction zones, cool oceanic crustal material from the Earth's surface descends into the warm mantle. This results in a cooling of the fore-arc regions, as reflected by low surface heat flow (<40 mW m^{-2}) observed over many fore arcs [e.g., *Lewis et al.*, 1988; *Ziagos et al.*, 1985; *Springer and Forster*, 1998; *Yamano*, 1995] and as indicated by the inferred existence of serpentine in the fore-arc mantle wedge, which is stable only below about 700°C [*Hyndman and Peacock*, 2003, and references therein]. There is a dramatic change to high temperatures just seaward of the volcanic arc. Most subduction zones are characterized by margin-parallel active volcanoes, the volcanic arc. Although limited slab melting may occur in a few regions [e.g., *Defant and Drummond*, 1990], the majority of arc magma appears to be derived from partial melting of the mantle wedge above the subducting slab, induced by lowering of the mantle solidus by the upward infiltration of fluids dehydrated from the slab [e.g., *Gill*, 1981; *Ulmer*, 2001; *Stern*, 2002]. Geochemical arguments indicate arc magma temperatures of at least 1200°C, and possibly greater than 1300°C, in the magma source regions at 60–100 km depth [e.g., *Tatsumi et al.*, 1983; *Ulmer*, 2001; *Kelemen et al.*, 2003; *Peacock*, 2003, and references therein]. High temperatures in the shallow subarc mantle are also well demonstrated by high surface heat flow, low mantle seismic velocities and high mantle seismic attenuation [e.g., *Zhao*, 2001].

[3] Such high temperatures in the mantle above the heat sink of a subducting plate are extraordinary. It has been argued that local sources of heat, including shear heating along the subducting plate surface, heat associated with metamorphism, and radiogenic heat production, are insufficient to significantly elevate temperatures in the mantle wedge [e.g., *McKenzie*, 1969; *Andrews and Sleep*, 1974; *Peacock*, 1996 and references therein]. The current consensus is that mantle flow carries heat from outside the subduction zone region into the mantle wedge.

[4] The main driving forces for flow in the back-arc mantle are thermal buoyancy and viscous coupling between the subducting slab and surrounding mantle (corner flow) (Figure 1). Despite the large number of modeling studies of mantle dynamics at a subduction zone, neither the geometry nor vigor of back-arc mantle flow are well defined [*Peacock*, 1996, 2003]. The high mantle temperatures associated with arc

[1]School of Earth and Ocean Sciences, University of Victoria, Victoria, British Columbia, Canada.
[2]Now at Department of Oceanography, Dalhousie University, Halifax, Nova Scotia, Canada.
[3]Pacific Geoscience Centre, Geological Survey of Canada, Sidney, British Columbia, Canada.

0148-0227/06/2005JB004024$09.00

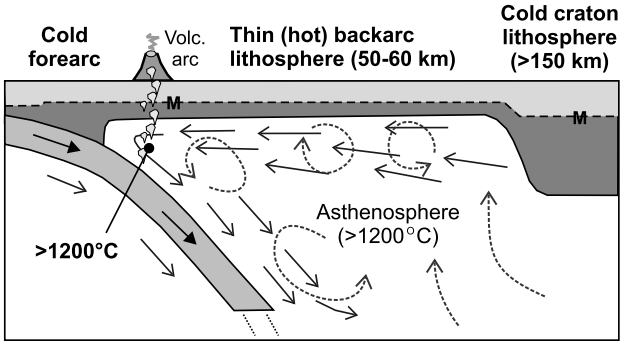

Figure 1. Schematic cross section through a continental subduction zone. The main driving forces for back-arc mantle flow are viscous coupling with the subducting slab (solid arrows) and thermal buoyancy (dashed arrows). The landward limit of the back arc in some areas is an Archean craton.

volcanism place one critical constraint on back-arc mantle dynamics; flow must carry enough heat to maintain at least 1200°C in the subarc mantle. A second important restriction on flow dynamics comes from constraints on shallow mantle temperatures well behind the volcanic arc.

[5] Early inferences of back-arc thermal structure came from subduction zones in the western Pacific, e.g., NE Japan, Kuril, Izu-Bonin and Tonga, where anomalously high heat flow (>80 mW m^{-2}) is observed for hundreds of kilometers behind the volcanic arc [*Vacquier et al.*, 1966; *McKenzie and Sclater*, 1968; *Oxburgh and Turcotte*, 1968; *Sclater*, 1972]. As most of these back arcs have undergone significant recent crustal extension and, in places, back-arc spreading that produced new oceanic crust, the high heat flow has been primarily attributed to extension [e.g., *Karig*, 1971; *Sleep and Toksoz*, 1971; *Watanabe et al.*, 1977]. However, the thermal effects of both extensional thinning of the lithosphere and hot mantle upwelling at back-arc spreading centers mask the underlying thermal effects related to subduction.

[6] In this study, we document observations indicating that nearly all subduction zones are characterized by a hot back-arc mantle, not just those that have undergone recent extension. We focus on back arcs where there has been a long history of subduction and where there is no ongoing extension at thermally significant rates, i.e., more than a few millimeters per year [e.g., *Jarvis and McKenzie*, 1980], using seismic, GPS velocity, and geological data. All our areas are more than 100 km from regions that are currently undergoing significant extension; *Morgan* [1983] concluded that the thermal effects of extension propagate only a short distance from the region of largest extension. We have also reviewed the tectonic history of each area to ensure that there has been no thermally significant extension within the last 50 Myr, since the thermal effects of extension decay with a time constant of about 50 Myr [*Jarvis and McKenzie*, 1980]. We have identified ten circum-Pacific back arcs that fit these criteria and where there are adequate constraints on the thermal structure (Figure 2). All but one of the back arcs in our study are continental; the exception is the Aleutian back arc.

[7] We first describe the types of observations that constrain shallow back-arc mantle temperatures. We then present our compilation for the ten back arcs in our study, followed by a brief summary of thermal data for other back arcs, including those with recent extension and those of former subduction zones. In nearly all cases, the observations indicate high temperatures in the shallow back-arc mantle. The exception is the Peru region of South America, where there is a shallow flat subducting slab that appears to restrict mantle wedge flow. We end with a discussion of the implications of a uniformly hot back arc for mantle dynamics.

2. Observational Constraints on Back-Arc Temperatures

[8] Direct measurement of temperature is limited to the upper few kilometers of the Earth's crust. Temperature estimates at greater depth require indirect methods, such as surface heat flow and radiogenic heat production, mantle seismic velocity from refraction and tomography studies, and thermobarometry studies of mantle xenoliths. The mantle temperatures inferred from each type of observation have considerable uncertainty. However, by using two or more independent techniques, more robust estimates may be obtained. Below we review the temperature constraints and their uncertainties. As a calibration for each method, we use the well-constrained thermal structure of Archean cratons. We note that there are only small differences in uppermost mantle temperatures between the cratons and stable Paleozoic platforms.

2.1. Surface Heat Flow

[9] One main constraint on uppermost mantle temperature comes from surface heat flow and radioactive heat generation data. Surface heat flow for continental regions reflects the combination of radiogenic heat produced in the

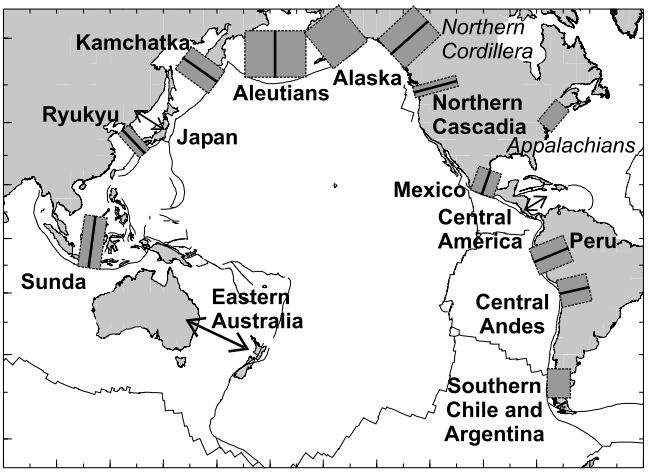

Figure 2. Back arcs examined in this study are shown with grey boxes (line shows the location of heat flow profiles). Arrows indicate regions that appear to be hot but where the thermal structure has not been examined in detail. Regions labeled in italics represent former back arcs, where subduction has ceased within the last 300 Myr.

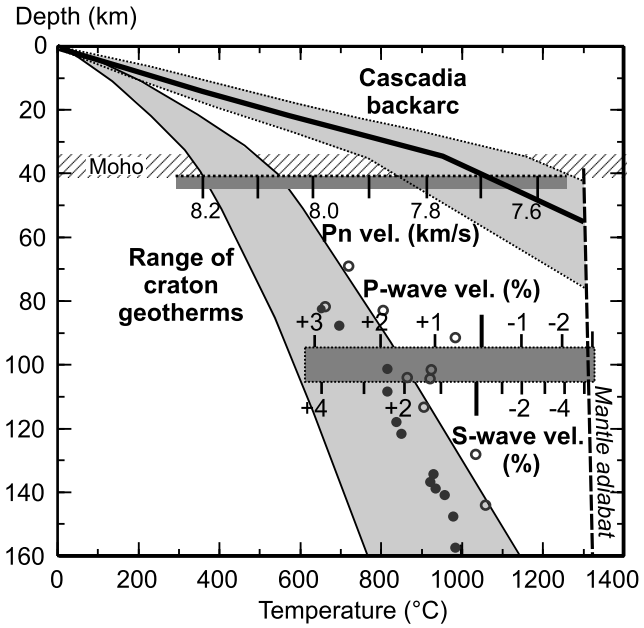

Figure 3. Constraints on mantle temperatures from P_n velocities [*Black and Braile*, 1982] and velocities from seismic tomography [*Goes et al.*, 2000]. Also shown is the inferred geotherm for the northern Cascadia back arc (see text) and Archean cratons from surface heat flow–heat generation and mantle xenonolith thermobarometry studies (solid circles, *Russell and Kopylova* [1999]; open circles, *MacKenzie and Canil* [1999]).

crust and heat flux from the underlying mantle. For areas with measurements of surface heat flow and near-surface heat production, the temperature as a function of depth can be calculated from the heat conduction equation, assuming steady state and thermal parameters (thermal conductivity and radiogenic heat production) that vary only with depth [e.g., *Chapman*, 1986]. The main uncertainties in the calculated geotherm come from (1) uncertainties in the depth distribution of crustal radiogenic heat production [*Rudnick and Fountain*, 1995; *Rudnick et al.*, 1998], (2) the poorly constrained decrease in thermal conductivity with increasing temperature [e.g., *Sass et al.*, 1992; *Clauser and Huenges*, 1995], and (3) possible radiative heat transfer at high temperatures (>900°C) [*Clauser and Huenges*, 1995]. Using reasonable variations in each of these parameters, we estimate that there is a 20% uncertainty in the calculated geotherm [*Flück*, 2003; *Currie*, 2004].

[10] In general, Archean cratons are characterized by low surface heat flow, 42 ± 10 mW m^{-2} [e.g., *Nyblade and Pollack*, 1993; *Artemieva and Mooney*, 2001; *Jaupart et al.*, 1998; *Jaupart and Mareschal*, 1999; *Mareschal and Jaupart*, 2004]. Figure 3 shows the range of lithosphere temperatures for Archean cratons from surface heat flow–heat generation studies [*Jaupart et al.*, 1998; *Jaupart and Marechal*, 1999; *Artemieva and Mooney*, 2001]. Stable Paleozoic platforms have only slightly higher average heat flows [e.g., *Chapman and Pollack*, 1975].

[11] We have compiled available surface heat flow data for each back arc in our study. We have not attempted a rigorous quality selection, but where possible we have used the original data sources, allowing us to reject values that are reported to be of poor quality (i.e., estimated uncertainties greater than 20%). In a few cases, we have used the *Global Heat Flow Database* (data available at http://www.heatflow.und.edu; see also *Pollack et al.* [1993]). Only limited quality constraints are available from the database and we have only rejected the few heat flow values that are unreasonably low (<10 mW m^{-2}) or unreasonably high (>120 mW m^{-2}), or that we conclude have large uncertainties. For example, we exclude measurements with a small number of temperature gradient or thermal conductivity measurements at the site, shallow boreholes, or obvious temperature disturbances.

2.2. Mantle Seismic Velocities

[12] A second constraint on the uppermost mantle temperatures comes from seismic velocities. In the mantle, seismic velocity is primarily controlled by temperature; composition and anisotropy are generally second-order effects [e.g., *Goes et al.*, 2000; *Wiens and Smith*, 2003]. In the back-arc mantle, seismic velocities may also be affected the presence of partial melt, as well as water and other volatiles released from the subducting slab [e.g., *Goes et al.*, 2000; *Goes and van der Lee*, 2002; *Wiens and Smith*, 2003]. Both water and melt will act to decrease seismic velocities, and thus the back-arc mantle temperatures that we estimate may be too high, particularly those inferred using S waves [e.g., *Dixon et al.*, 2004].

[13] In our compilation, we include two constraints on upper mantle seismic velocity: P_n uppermost mantle velocity from seismic refraction studies and P and S wave velocities at depths of 50–150 km from seismic tomography. Seismic attenuation, Q, also is very sensitive to temperature. We find that back-arc estimates of upper mantle Q are consistently low, as expected for high temperatures [e.g., *Barazangi et al.*, 1975; *Flanagan and Wiens*, 1994; *Wiens and Smith*, 2003], but the temperature inferences do not yet appear to be sufficiently quantitative to provide much additional constraint on thermal structure.

2.2.1. P_n Velocities

[14] P_n waves are seismic head waves that refract along the Moho and thus are sensitive to the mantle velocity immediately below the Moho. P_n velocities can be measured with high precision (±0.1 km s^{-1}) using local seismic refraction profiles (reversed or multishot/multireceiver profiles must be used to obtain the greatest accuracy), or through P_n tomography studies using regional earthquakes. From a study of P_n velocity and lithosphere thermal structure, mainly from heat flow data for North America, *Black and Braile* [1982] proposed an empirical relation between P_n velocity (km s^{-1}) and Moho temperature (T_m, in °C):

$$P_n = 8.456 - 0.000729T_m \quad (1)$$

The relationship between P_n velocity and T_m is shown on Figure 3. As discussed by *Hyndman and Lewis* [1999], the temperature coefficient (−0.000729 km s^{-1} $°C^{-1}$) is in good agreement with that obtained in laboratory studies of

seismic velocity [e.g., *Christensen*, 1979; *Karato*, 1993], although there is a significant uncertainty due to anelastic effects. The temperature constant (velocity at 0°C of 8.456 km s^{-1}) also has significant uncertainty. These factors, as well as the effects of compositional variations and anisotropy, result in ±150°C uncertainty in the calculated Moho temperatures.

[15] For Archean cratons that we use for method calibration, the observed P_n velocities are high, generally between 8.1 to 8.2 km s^{-1}, with some values as high as 8.3 km s^{-1} [e.g., *Christensen and Mooney*, 1995; *Levshin et al.*, 2001; *Perry et al.*, 2002]. For a craton P_n velocity of 8.1–8.2, equation (1) predicts a Moho temperature at 40 km depth of 350–490°C, in good agreement with the published geotherms from heat flow (Figure 3). In contrast, as we document below, most back arcs have P_n velocities of 7.8–7.9 km s^{-1} which suggests temperatures of 800–900°C.

2.2.2. Seismic Tomography

[16] Upper mantle velocities from regional and global P wave and S wave tomography have low spatial resolution, but have excellent regional coverage. Recent studies have used sophisticated techniques to infer mantle temperatures from seismic tomography data, taking into consideration compositional variations and the nonlinearity introduced by anelasticity [e.g., *Goes et al.*, 2000; *Goes and van der Lee*, 2002]. In our compilation, we use the temperature-velocity relation of *Goes et al.* [2000], assuming a primitive garnet peridotite mantle composition and the anelasticity model of *Sobolev et al.* [1996] (Figure 3). Estimated uncertainties in the temperatures inferred from this relation are about 100°C (S. Goes, personal communication, 2005).

[17] In global tomography images, Archean cratons appear as regions of high seismic velocity, where P wave velocities are typically 2–3% fast [e.g., *Bijwaard et al.*, 1998; *Bijwaard and Spakman*, 2000] and S wave velocities are 3–4% fast [e.g., *Zhang and Tanimoto*, 1993; *Grand*, 1994; *van der Lee and Nolet*, 1997; *van der Lee and Frederiksen*, 2005], relative to average mantle velocities. Some of the high velocity may be due to chemical depletion of the subcratonic mantle, which increases seismic velocities by 1–2% relative to a primitive mantle composition [e.g., *Jordan*, 1978; *Shapiro and Ritzwoller*, 2004]. The remaining high-velocity anomaly is primarily attributed to low temperature. Using both P and S wave tomography, temperatures of 700–900°C at ~100 km depth are inferred for Archean cratons in North America [*Goes and van der Lee*, 2002], Europe [*Goes et al.*, 2000], and Australia [*Goes et al.*, 2005].

[18] In our study, we focus on the regional P wave and S wave velocity structure of the back-arc mantle between 50 and 150 km depth. For details about smaller-scale lateral variations in velocity, the reader is referred to the individual publications. The majority of studies report tomography results as a velocity perturbation with respect to the reference model used in the data inversion. The reference models are usually based on global average mantle velocities (e.g., model ak135 [*Kennett et al.*, 1995]). However, some studies use locally derived reference models [e.g., *Zhao et al.*, 1995]. In order to compare the various studies, we have converted the published tomography results into an absolute velocity and then calculated the percentage perturbation relative to model ak135, i.e., V_P of 8.05 km s^{-1} and V_S of 4.5 km s^{-1} at ~100 km depth [*Kennett et al.*, 1995].

2.3. Mantle Xenoliths

[19] Thermobarometry measurements on mantle xenoliths provide excellent local constraints on the pressure-temperature conditions at the xenolith source region, especially using garnets exhumed in cratonic kimberlites. There are a number of uncertainties, including the temperature and pressure coefficients of the chemical equilibria, whether the chemical equilibria represent current conditions, chemical changes associated with exhumation, and whether the sites of kimberlites are representative of larger areas, but the results appear to be reliable. Numerous thermobarometry studies of mantle xenoliths from the Archean North America craton [e.g., *MacKenzie and Canil*, 1999; *Russell and Kopylova*, 1999] and other Archean cratons [e.g., *Rudnick et al.*, 1998] indicate low temperatures to large depths, in good agreement with temperatures inferred from surface heat flow and mantle seismic velocities (Figure 3).

[20] Unfortunately, where the mantle is hot, the key indicators used to determine pressure (e.g., garnet) are often absent. Other mineral chemical equilibria give well-constrained temperatures, but the large uncertainties in the pressure commonly provide only a rough indicator of the minimum origin depth. If there are a large number of xenoliths having a wide temperature range, the samples with the minimum temperature may be interpreted as originating from just below the Moho [e.g., *Harder and Russell*, 2006]. It is important to note that xenoliths provide point measurements of the lithosphere. They may be biased by only providing information for the special areas and conditions where xenoliths occur.

2.4. Other Observations

[21] There are a number of other semiquantitative observations that can be used as indicators of the thermal structure of the uppermost mantle:

[22] 1. The occurrence of basaltic (i.e., mantle-derived) volcanism suggests that temperatures in the shallow mantle are near the solidus [e.g., *Stern et al.*, 1990]. Cenozoic volcanic rocks are common in current back arcs. In contrast, recent basaltic volcanic fields are very rare for cratons (e.g., for North America craton [*Wheeler and McFeely*, 1991]).

[23] 2. The effective elastic thickness (T_e), inferred from studies of the wavelength of surface flexure using gravity and topography data, is primarily temperature-controlled, i.e., loosely described as the depth to the "brittle-ductile transition" (~400°C for granitic crust and ~600°C for basaltic crust and mantle rocks) [e.g., *Flück et al.*, 2003]. As an example, the effective elastic thickness for the Archean North America craton is generally greater than 80 km [e.g., *Flück et al.*, 2003; *Wang and Mareschal*, 1999], whereas it is generally less than 20 km for the Cordillera back arc.

[24] 3. Surface elevation and crustal thickness data can be used as a proxy for the uppermost mantle temperature because of the reduction in mantle density with increasing temperature. For example, the North America craton has generally low elevation (<500 m) and average crustal thickness (~40 km), consistent with cool lithosphere temperatures, in contrast to the Cordillera which generally has

Table 1. Summary of Observations for the Present-Day and Former Back Arcs in the Compilation[a]

Region (Arc–Back Arc)	Back Arc Width, km	Surface Heat Flow, mW m^{-2}	P_n Velocity, km s^{-1}	Vp Tomography,[b] %	Vs Tomography,[b] %	Basaltic Volcanism	P-T From Mantle Xenoliths
Cascadia–SW Canada	500	75 ± 15[c]	7.8–7.9	−1 to −3	−3 to more than −8	yes	900°C (35 km) to 1300°C (70 km)
South America–South Chile/Argentina	>400				−2.5 to −4.5	yes	970°C (60 km) to 1160°C (75 km)
South America–central Andes	400	85 ± 16	8.0–8.1[d]	−2 to −3	−4 to more than −10	yes	1000°C (45 km)[e]
South America–Peru (flat slab)		~50					
Mexico	>250	72 ± 17	7.8 ± 0.2	−1 to −3	−3 to −4		
Alaska–Bering Shelf/continental Alaska	>800		7.8–8.0	−1 to −3		yes	850–1030°C (45 km)
Aleutian–Bering Sea	>900	75 ± 15[f]	7.8–8.0	−1 to −2		yes	850–1030°C (45 km)
Kamchatka–Sea of Okhotsk	>700	70 ± 18	7.8–7.9	−2	−4 to more than −7		
Ryukyu–Korea	>600	69 ± 16	7.8–8.0	−2			
Sunda–Borneo	>800	76 ± 18		−2	−4	yes	
Northern Canadian Cordillera (~42 Ma)	600	76 ± 21[c]	7.8–7.9	−1 to −2	−3 to −4	yes	805°C (35–40 km)
Appalachians (~260 Ma)		50–60			−1 to +1		
Archean craton (average)		42 ± 10	8.1–8.2	+2 to +3	+3 to +4	none	700°C (80 km)

[a]See text for references.
[b]Tomography velocities reported as a perturbation relative to average mantle velocities at depths of 50–150 km [from *Kennett et al.*, 1995].
[c]Heat flow has been corrected to an upper crustal heat generation of 1.3 μW m^{-3} (see text).
[d]The high P_n velocity may be partially due to the pressure effects as the Moho is at a depth of ~65 km.
[e]Xenoliths erupted at 90 Ma; crustal thickness at that time was ~35 km.
[f]Heat flow has been corrected for the effects of sedimentation [*Langseth et al.*, 1980].

high elevations (1.5–2 km) and thin crust (32–35 km), indicating high temperatures [e.g., *Hyndman and Lewis*, 1999].

3. Thermal Structure of Present-Day Back Arcs With No Significant Extension

[25] For each back arc in Figure 2, we document the available constraints on the temperature of the uppermost mantle using the techniques described above. Table 1 provides a summary of our compilation. We start with thermal constraints for the northern Cascadia back arc, where the large number of high-quality observations allows the geotherm to be well constrained. This geotherm is then used for comparison to the other back arcs.

3.1. Northern Cascadia

[26] Subduction along the Cascadia margin has been continuous for at least 200 Myr [e.g., *Monger and Price*, 2002]. In our study, we focus on the northern part of the Cascadia back arc (48–51°N), which has been tectonically quiescent since the early Cenozoic [e.g., *Gabrielse*, 1992]. The most recent significant tectonic activity was a short-lived (<10 Myr) period of extension in the Eocene in a small area of southeast British Columbia, but it has been concluded from thermochronologic studies of core complexes and thermal modeling that this area was hot well before extension [*Liu and Furlong*, 1993].

[27] We limit our study to the region north of 48°N. In the southern Cascadia back arc, there are large differences in geological structure and late Cenozoic tectonics, and the thermal regime is complicated by both the proximity of the Yellowstone hot spot and by current extension in the Basin and Range province. We note that heat flow, mantle seismic velocities, and other temperature indicators suggest that the mantle thermal structure here is similar to that of the northern Cascadia back arc [e.g., *Roy et al.*, 1972; *Blackwell et al.*, 1990a, 1990b; *Lowry and Smith*, 1994; *Blackwell and Richards*, 2004]. As argued by *Blackwell* [e.g., 1969, 1978], the entire Cordilleran mountain belt of the northwest United States appears to be uniformly hot and the high temperatures of the Basin and Range province are not simply due to extension. We further note that California and northern Mexico appear to be similarly hot [e.g., *Goes and van der Lee*, 2002; *Dixon et al.*, 2004], although subduction terminated at 10–30 Ma. In section 6, we discuss the cooling of former back arcs.

[28] At the northern Cascadia subduction zone, surface heat flow is high in the volcanic arc region and for 500 km east into the back arc [*Davis and Lewis*, 1984; *Lewis et al.*, 1988, 1992; *Blackwell et al.*, 1990a, 1990b; *Hyndman and Lewis*, 1999; *Flück*, 2003] (Figure 4a). The back-arc heat flow increases eastward from ~70 mW m^{-2} in the west to >100 mW m^{-2} in the east (Figure 4b). Numerous high-quality measurements of near-surface radiogenic heat production show that the eastward increase in surface heat flow is correlated with an eastward increase in radiogenic heat production, from 1 μW m^{-3} in the west to 3.6 μW m^{-3} in the east, such that the deep thermal structure is nearly uniform across the back arc, with a reduced heat flow of ~60 mW m^{-2} [*Lewis et al.*, 1992; *Hyndman and Lewis*, 1999]. To aid in the comparison with the heat flow of other back arcs, we have corrected the northern Cascadia heat flow to that for a common upper crustal heat production of 1.3 μW m^{-3}, assuming uniform heat production in the upper 10 km of the crust. After correction, the surface heat flow across the Cascadia back arc is relatively uniform, 75 ± 15 mW m^{-2}.

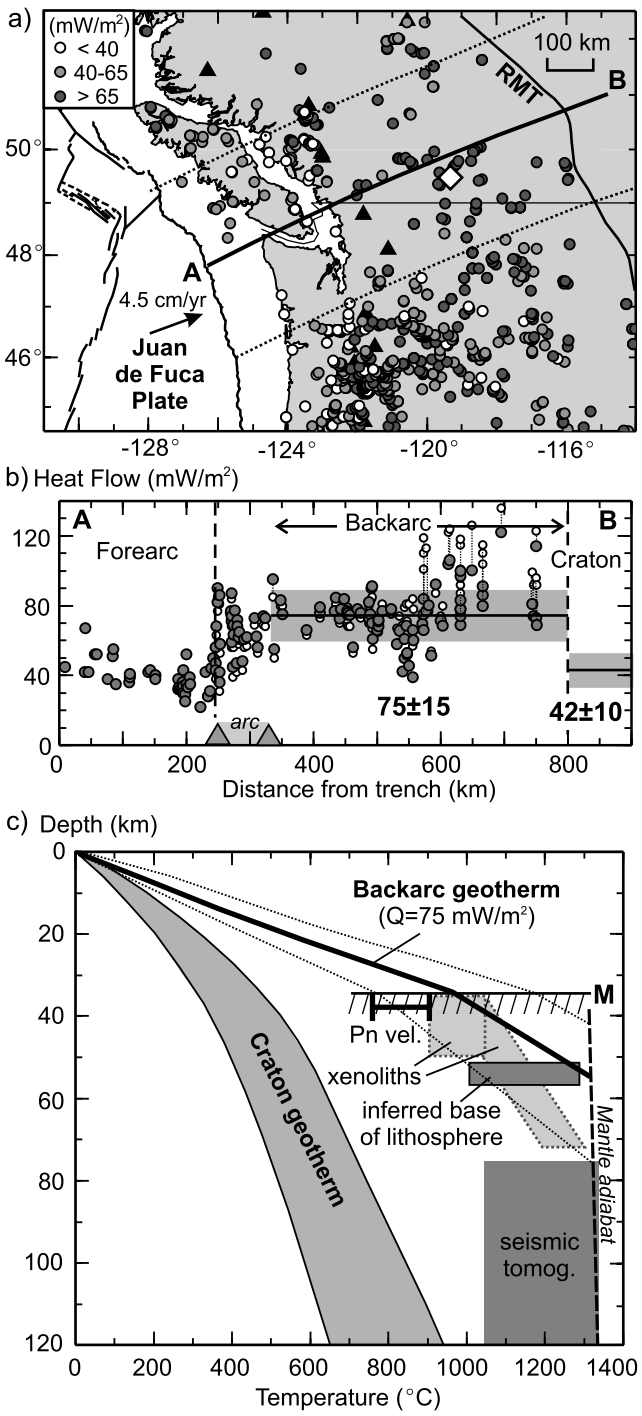

Figure 4. (a) Heat flow data for the northern Cascadia subduction zone. The white diamond indicates where mantle xenoliths have been recovered. Solid triangles are active arc volcanoes. The eastern limit of the back arc is the Rocky Mountain Trench (RMT). The solid line is the heat flow profile location; dotted lines show the profile data width. (b) Heat flow profile along line A-B. The measured heat flow values (open circles) have been corrected for variations in near-surface heat generation (solid circles) (see text). (c) Back-arc geotherm from surface heat flow (dotted lines are 20% uncertainty) and other thermal constraints.

[29] We have calculated a geotherm for this surface heat flow and heat generation, following the procedure of *Chapman* [1986]. We use a three-layer model, consisting of a 10 km thick upper crust, 25 km thick lower crust, and an upper mantle. For the crust and mantle, we use the temperature-dependent thermal conductivity of *Sass et al.* [1992] [see also *Lewis et al.*, 2003]. The heat productions are 1.3, 0.6, and 0.02 μW m^{-3} for the upper crust, lower crust and mantle, respectively, consistent with estimates of crust and mantle heat production [e.g., *Chapman*, 1986; *Rudnick and Fountain*, 1995; *Rudnick et al.*, 1998; *Hyndman and Lewis*, 1999].

[30] Figure 4c shows the calculated geotherm for the northern Cascadia back arc. This geotherm is similar to those from previous heat flow–heat generation studies for this area [e.g., *Lewis et al.*, 1992; *Hyndman and Lewis*, 1999]. High temperatures in the uppermost mantle are predicted throughout the northern Cascadia back arc, with estimated temperatures at the Moho (~35 km depth) greater than 900°C. As noted above, these temperatures may be somewhat too high because we neglect radiative thermal conduction at high temperatures, but it is difficult to obtain Moho temperatures less than 800°C with reasonable parameters. These temperatures are much higher than the solidus temperature for most crustal rocks that contain at least a small amount of water. As there is no obvious geological or geophysical evidence for significant melting of the lower crust in this region, this may indicate that the lower crust is mafic and dry.

[31] Additional constraints on uppermost mantle temperatures come from seismic velocity studies. Extensive seismic refraction data for the northern Cascadia back arc, especially from the Lithoprobe program, indicate consistently low P_n velocities of 7.8–7.9 km s^{-1} [*Zelt and White*, 1995; *Clowes et al.*, 1995; *Burianyk and Kanasewich*, 1995], giving an estimated Moho temperature of 760–900°C (Figure 4c). This temperature is slightly lower that that determined from heat flow, but within the uncertainties of the methods. Seismic tomography studies have poor depth resolution but show that, relative to average mantle velocities at 50–150 km depth, the upper mantle throughout the northern Cascadia back arc has P wave velocities that are 1–3% slow [e.g., *Bijwaard and Spakman*, 2000] and S wave velocities that are 3% to more than 8% slow [e.g., *Grand*, 1994; *van der Lee and Nolet*, 1997; *Frederiksen et al.*, 2001; *van der Lee and Frederiksen*, 2005] (Figure 5a), suggesting mantle temperatures greater than 1150°C at depths greater than 50 km. Small amounts of water and perhaps partial melt are expected to have only a small effect on P wave velocities. However, the extremely low observed S wave velocities likely reflect the combined effects of high temperatures and the presence of a small amount (<2%) of water, other volatiles and partial melt [e.g., *van der Lee and Nolet*, 1997; *Frederiksen et al.*, 2001; *Goes and van der Lee*, 2002; *Dixon et al.*, 2004].

[32] Upper mantle xenoliths have been recovered from several localities in the northern Cascadia back arc. Three suites of peridotite xenoliths from the central back arc yield temperatures of 1000°C at ~40 km depth, increasing to 1300°C at 60–70 km depth [*Ross*, 1983] (Figure 4c). A recent study of xenoliths from the same region indicates

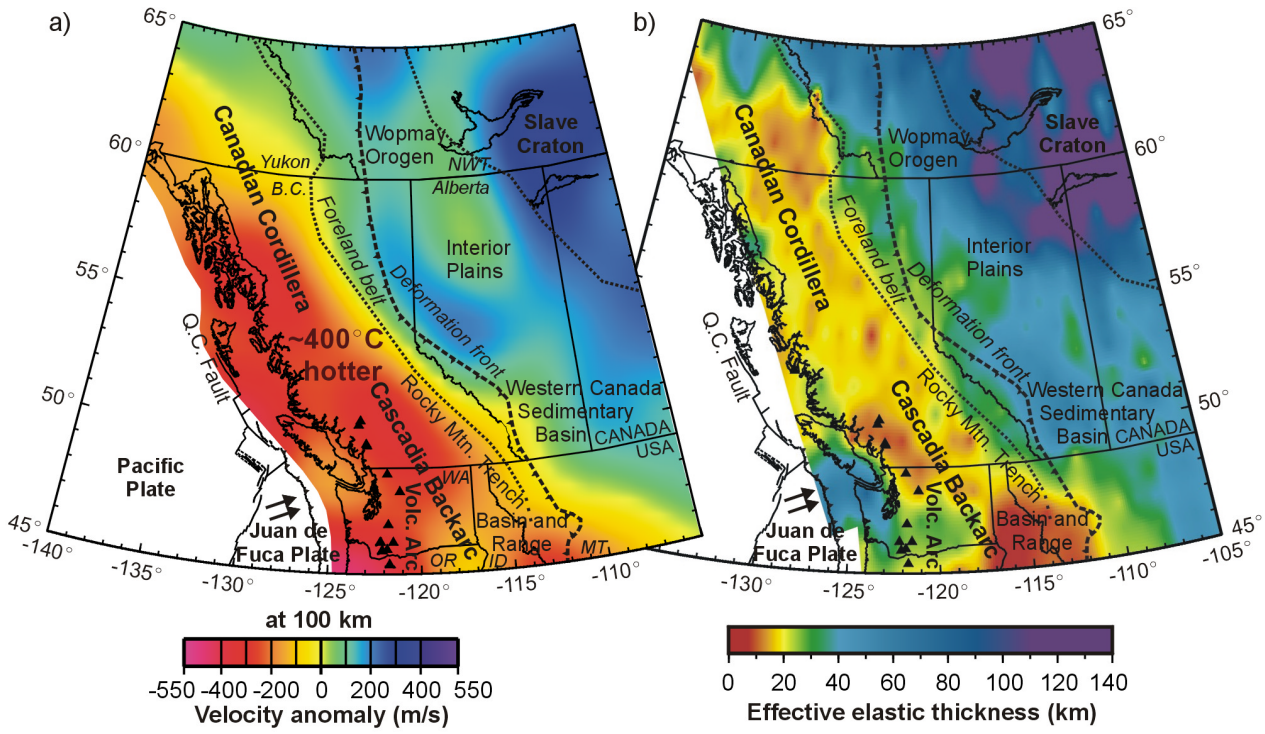

Figure 5. (a) S wave tomography velocities at ~100 km depth for western Canada [*van der Lee and Frederiksen*, 2005]. Velocity anomalies are in m s^{-1} relative to a reference velocity of 4500 m s^{-1}. (b) Effective elastic thickness for western Canada from topography and gravity. Canadian data are from *Flück et al.* [2003]; U.S. data are from *Lowry and Smith* [1995].

temperatures of 900–1040°C at 1.2–1.6 GPa (35–50 km depth) [*Saruwatari et al.*, 2001].

[33] For the Cascadia back arc, the surface elevation is generally 1500–2000 m, whereas the crust is thin, averaging ~33 km [e.g., *Clowes et al.*, 1995; *Burianyk et al.*, 1997]. As seismic velocities indicated that the crust is of average density, the high elevations appear to be related to a low-density mantle [*Lowe and Ranalli*, 1993; *Hyndman and Lewis*, 1999]. *Hyndman and Lewis* [1999] show that the density reduction associated with high upper mantle temperatures (similar to those in Figure 4c) can explain the observed back-arc thin crust and high elevations.

[34] Several observations indicate that the base of the lithosphere is at shallow depths throughout the northern Cascadia back arc. *Clowes et al.* [1995] report an upper mantle reflector at ~50 km depth in seismic data for the central back arc, which they interpret as the base of the lithosphere. An earlier surface wave study shows a low-velocity layer, interpreted to be the asthenosphere, with its upper boundary at 50–55 km depth [*Wickens*, 1977]. In addition, upper mantle xenoliths record a rapid downward increase in strain rate at depths of 50–60 km, which may indicate a transition from rigid lithosphere to convecting asthenospheric mantle [*Ross*, 1983]. A lithosphere thickness of 50–60 km is similar to the inferred intersection of the conductive geotherm discussed above with a standard 1300°C mantle adiabat (Figure 4c).

[35] High temperatures in the shallow back-arc mantle are also indicated by (1) widespread sporadic Cretaceous to Recent basaltic volcanic centers, including the Chilcotin Plateau basalts and Wells Gray–Clearwater volcanic field [e.g., *Wheeler and McFeely*, 1991]; (2) an effective elastic thickness of less than 20 km throughout the entire region [*Flück et al.*, 2003] (Figure 5b); and (3) high electrical conductivity in both the lower crust and upper mantle, which is interpreted to reflect the presence of partial melt at shallow depth and a thin lithosphere [*Soyer and Unsworth*, 2006, and references therein].

[36] Taken together, the observations for the northern Cascadia back arc indicate a uniformly hot upper mantle for 500 km east of the volcanic arc, with no significant lateral variation. We estimate temperatures of 800–1000°C at the Moho (~35 km depth) and a lithosphere thickness of 50–60 km, where temperatures are estimated to be ~1200°C (Figure 4c). The high temperatures are especially surprising as the northern Cascadia back arc is bounded on the east by the edge of the unextended North America craton, which is much cooler. The eastern limit of the back arc is concluded to coincide with the Rocky Mountain Trench, based on rapid changes in lithosphere properties, thermal regime, and deformation styles across this boundary [*Lowe and Ranalli*, 1993; *Hyndman and Lewis*, 1999]. Earlier studies suggested that the Cascadia back arc, as well as regions to the north and south, overlie a large-scale upwelling of anomalously hot mantle [e.g., *Gough*, 1986]. Our current compilation supports an explanation of convective upwelling in the mantle, but suggests that it is not unique to this region. As shown below, high temperatures

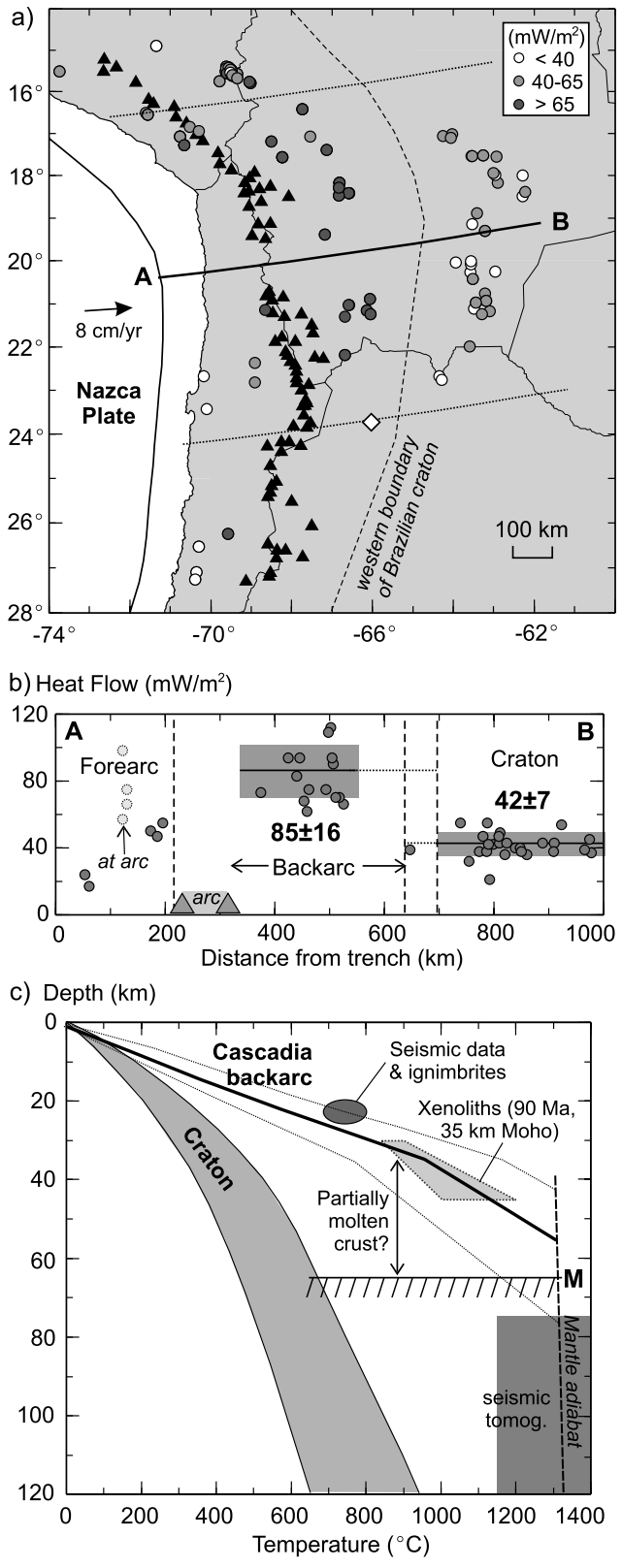

Figure 6. (a) Map of the central Andean part of the South America subduction zone. The white diamond shows the location of mantle xenoliths (erupted at 90 Ma). (b) Heat flow profile along line A-B. (c) Inferred thermal structure for the central Andes back arc. The well-constrained Cascadia and Archean craton geotherms are shown for comparison.

are found in most other back arcs, suggesting that a hot back arc may be a characteristic feature of subduction zones and may be a direct result of back-arc mantle dynamics associated with the subduction process [e.g., *Davis and Lewis*, 1984].

3.2. Southern South America–Chile and Argentina (South of 35°S)

[37] The back arc of the southernmost part of the South America subduction zone (south of 35°S) appears to be fairly inactive, with only mild margin-normal compression [e.g., *Klotz et al.*, 2001]. Although there are no surface heat flow measurements for this region, high geothermal gradients (>30°C km^{-1}) have been measured in oil exploration wells in the back arc, suggesting high surface heat flow and high temperatures at depth [*Hamza and Munoz*, 1996]. Regional seismic tomography shows S wave velocities 2.5–4.5% slower than average mantle at depths of 60–150 km [*Robertson Maurice et al.*, 2003], consistent with temperatures of 1150–1300°C. In addition, seismic data indicate that lithosphere is only ~60 km thick [*Robertson Maurice et al.*, 2003]. The back arc is also characterized by sporadic Plio-Quaternary basaltic volcanism, particularly south of 39°S [*Stern et al.*, 1990]. Upper mantle xenoliths from the Pali-Aike basalt field (~52°S, 70°W) yield temperatures of 970°C at 1.9 GPa (~60 km depth), increasing to 1160°C at 2.4 GPa (~75 km depth) [*Stern et al.*, 1999]. The back-arc thermal structure may be affected by a slab window produced by the subduction of the Chile Rise spreading center at ~46°S. With the absence of a slab below this region, hot mantle from below may enter, locally increasing the wedge temperatures near the window. However, it is difficult to explain the inferred regionally extensive high temperatures solely by the slab window mechanism.

3.3. South America–Central Andes

[38] Along the central Andean segment of the South America subduction zone (15–28°S), the back-arc strain regime is dominated by shortening [e.g., *Allmendinger et al.*, 1997; *Klotz et al.*, 2001, and references therein]. Surface heat flow values are consistently high throughout the arc and back-arc regions, averaging 85 ± 16 mW m^{-2} [*Hamza and Munoz*, 1996; *Springer and Forster*, 1998] (Figure 6). The measured K, Th, and K contents in exposed basement sections in the central Andes (21–27°S) indicate a near-surface radiogenic heat production of 1.3 μW m^{-3} [*Lucassen et al.*, 2001], similar to our Cascadia reference value. The eastern limit of high heat flow coincides with the Brazilian Shield craton, where surface heat flow averages 42 mW m^{-2} [*Hamza and Munoz*, 1996], comparable to the North America craton.

[39] The back arc of the central Andes is made up of the Altiplano and Puna plateaus, which have elevations of 3.5–4 km and thick crust (60–75 km) [e.g., *Allmendinger et al.*, 1997]. At depths greater than 20 km, the crust is characterized by low P wave velocities (V_P), extremely low S wave velocities (V_S), a high V_P/V_S ratio, low density, and high electrical conductivity [*Schmitz et al.*, 1997; *Baumont et al.*, 2002; *Yuan et al.*, 2002; *Oncken et al.*, 2003, and references therein]. The low S wave velocities, high V_P/V_S ratio and high conductivity are interpreted to indicate a small amount

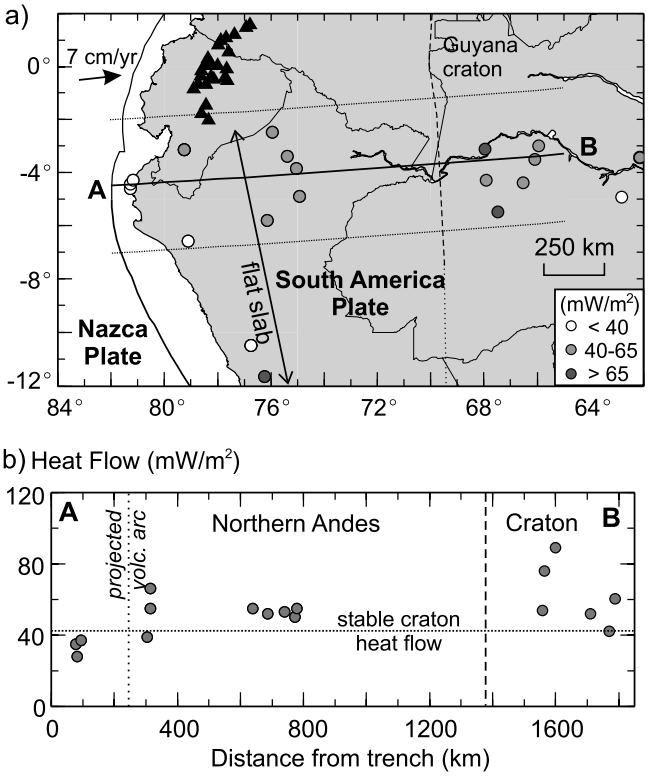

Figure 7. (a) Location map and (b) heat flow profile for the Peru region of the South America subduction zone. This area is characterized by a flat subducting slab at 100–125 km depth for >800 km east of the trench. There is no active volcanic arc along this part of the subduction margin.

of melt [*Yuan et al.*, 2002; *Oncken et al.*, 2003]. Further constraints on crustal temperature are provided by widespread late Miocene–early Pliocene ignimbrites throughout the back arc, which appear to have resulted from voluminous melting in the lower part of the thickened felsic crust [*Allmendinger et al.*, 1997]. Petrologic data indicates pre-eruptive midcrustal temperatures of 700–800°C [*Babeyko et al.*, 2002, and references therein]. Taken together, the observations give a temperature of ~800°C at 20–25 km depth (Figure 6c). Such midcrustal temperatures imply extremely high temperatures in the lowermost crust, unless the vertical gradient at depth is much reduced by radiative heat transfer or convection [*Babeyko et al.*, 2002].

[40] High surface heat flow and high crustal temperatures in the central Andes back arc have often been attributed to increased radiogenic heat production associated with the thick felsic crust. However, geological evidence shows that the Altiplano and Puna plateaus formed by tectonic shortening and thickening over the last 25 Myr [*Allmendinger et al.*, 1997]. For crustal thickening by pure shear, the surface heat flow first decreases and then increases as the crust is heated from below and by radiogenic heating. *Babeyko et al.* [2002] showed that the cooling effects of thickening should still dominate, due to the short time since thickening.

[41] In addition, it is unlikely that the crust will deform and thicken under available plate tectonic forces unless it is already hot and weak. Indeed, numerical models indicate that to produce the observed plateau topography, there must have been thermal weakening of the mantle across the entire width of the Altiplano prior to shortening [*Wdowinski and Bock*, 1994]. This conclusion is supported by lower crustal xenoliths from the Altiplano back arc that suggest that this region was hot before crustal thickening occurred. Thermobarometry studies of mafic granulite xenoliths erupted at 90 Ma from the Salta Rift (~24°S, 66°W) give temperatures of 850–900°C at 0.95–1.05 GPa (~30 km depth) [*Lucassen et al.*, 1999]. Upper mantle xenoliths from this location record temperatures of 1000–1200°C at 1.3–1.5 GPa (~45 km depth) [*Lucassen et al.*, 1999]. On the basis of these and other data, the Aliplano crust is inferred to have been ~35 km thick at 90 Ma, with Moho temperatures of ~900°C, i.e., similar to the current northern Cascadia back arc. High crustal temperatures before thickening and 10–20 Myr after thickening suggest a deep, long-lived heat source [e.g., *Babeyko et al.*, 2002]. This is consistent with observations that indicate present-day high temperatures in the shallow mantle.

[42] A limited seismic refraction study shows moderately low P_n velocities (8.0–8.1 km s^{-1}) below the Altiplano and an abrupt increase to 8.2 km s^{-1} at the Brazilian craton [*Baumont et al.*, 2001]. As the crustal thickness in this region is ~70 km, the somewhat higher P_n velocity relative to other back arcs may be partially due to higher pressure [e.g., *Christensen*, 1979], rather than lower temperatures. In addition, the refraction data are from an unreversed profile, which leads to large velocity uncertainties.

[43] Tomography data at ~100 km depth indicates that the entire width of the central Andes is characterized by P wave velocities that are 2–3% slow [*Bijwaard and Spakman*, 2000] and S wave velocity that are 4% to >10% slow [*van der Lee et al.*, 2001], relative to average mantle. Such low S wave velocities are likely the result of the combined effects of temperatures of at least 1200°C, as well as the presence of volatiles and partial melt [*van der Lee et al.*, 2001]. Surface wave dispersion studies also indicate a low-velocity upper mantle [*Baumont et al.*, 2002]. The back-arc upper mantle exhibits high seismic attenuation [*Haberland and Rietbrock*, 2001; *Schurr et al.*, 2003]. In addition, this region is characterized by the presence of Oligocene to Recent basaltic volcanic centers and fissure flows [*Allmendinger et al.*, 1997] and elevated $^3He/^4He$ ratios in groundwater [*Hoke et al.*, 1994], suggesting near-solidus temperatures in the uppermost mantle throughout the central Andes back arc.

3.4. Peru Flat Slab

[44] In our compilation, we find that the only regions with a cool back-arc mantle are where there is evidence for a flat subducting slab. In the Peru region of South America (2–15°S), the subducting Nazca oceanic plate is nearly horizontal at 100–125 km depth [*Cahill and Isacks*, 1992]. Heat flow near the coast is 30–40 mW m^{-2}, typical of fore arcs, but it is atypically low for a back arc, ~50 mW m^{-2}, farther inland across the northern Andes and onto the Guyana craton [*Hamza and Munoz*, 1996] (Figure 7). Seismic tomography indicates low S wave velocities in the mantle wedge, but the amplitude of the anomaly is smaller than to the north and south [*van der Lee et al.*, 2001]. In addition, there is no active volcanic arc, suggesting that the mantle is relatively cool.

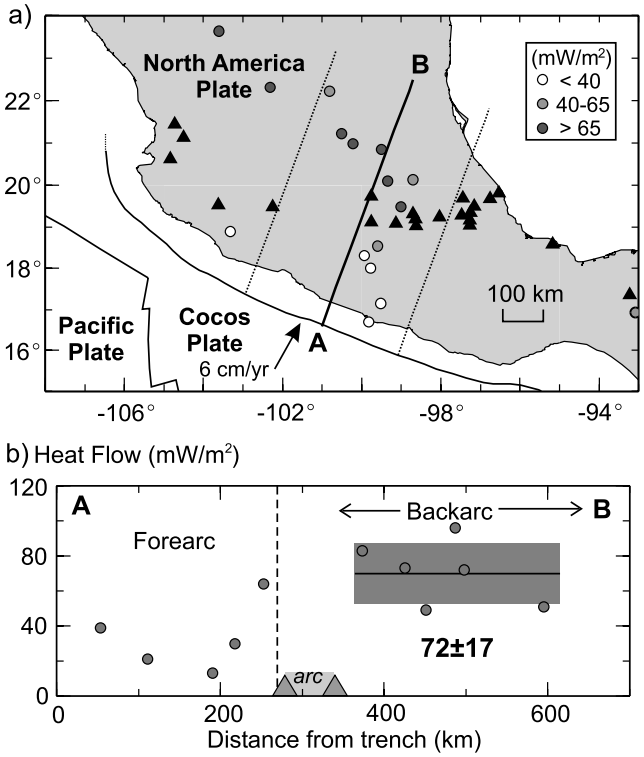

Figure 8. (a) Location map and (b) surface heat flow profile for the Mexico subduction zone.

[45] Another flat slab region occurs between 29 and 33°S. No heat flow data are available, but the absence of a volcanic arc suggests that the thin mantle wedge in this region is also cool. In addition, regional seismic tomography data show low P wave and high S wave mantle velocities above the flat slab, which are interpreted to reflect cool conditions and possible chemical alteration by slab-derived fluids [*Wagner et al.*, 2005].

3.5. Mexico

[46] The back arc of the Mexico subduction zone is characterized by generally diffuse seismicity and only localized extension west of our study area [e.g., *Rosas-Elguera et al.*, 1996; *Meschede and Frisch*, 1998]. In the central back arc, six surface heat flow measurements give a high average heat flow of 72 ± 17 mW m^{-2} over a distance of ~250 km behind the volcanic arc [*Ziagos et al.*, 1985] (Figure 8). Measurements of near-surface radiogenic heat production on 82 samples in the back arc yield an average heat production of 1.3 ± 0.6 μW m^{-3} [*Ziagos et al.*, 1985], similar to that used in the Cascadia geotherm calculation. A regional seismic study of northern and central Mexico indicates a P_n velocity of 7.8 ± 0.2 km s^{-1} [*Gomberg et al.*, 1988], which corresponds to temperatures of 900 ± 275°C. Seismic tomography studies at ~100 km depth show that P wave velocities are 1–3% slower than average mantle velocities [*Bijwaard and Spakman*, 2000] and S wave velocities are 3–4% slower [*Grand*, 1994; *van der Lee and Nolet*, 1997], suggesting temperatures greater than 1100°C [*Goes and van der Lee*, 2002]. High mantle temperatures are also indicated by high surface elevations (1500–3000 m), although the crust has a thickness of 35–40 km [*Gomberg et al.*, 1988, and references therein]. In addition, seismic studies show that the top of a low-velocity region in the mantle (taken as the base of the lithosphere) is at depths less than 70 km [*Gomberg et al.*, 1988].

3.6. Aleutians and Alaska

[47] We summarize observations for the Aleutian and Alaska back arcs together, as there is some overlap in the observational data. The Aleutian back arc west of the Bering Sea shelf edge is composed of oceanic crust, overlain by up to 4 km of sediments [*Langseth et al.*, 1980]. This part of the back arc was formed in the early Eocene (50–55 Ma), when subduction along the then-active Beringian margin (near the Bering Sea Shelf edge) jumped southwest to its present location, trapping a fragment of early Cretaceous (117–132 Ma) oceanic crust [*Cooper et al.*, 1992]. Recent (<20 Ma) back-arc spreading is confined to Komandorsky Basin, in the westernmost part of the back arc [*Cooper et al.*, 1992, and references therein]. The rest of the back arc is inactive, with no significant extension.

[48] High heat flow is found throughout the Aleutian back arc, averaging 63 ± 15 mW m^{-2} with no clear decrease with distance from the arc (*Langseth et al.* [1980] and data from http://www.heatflow.und.edu) (Figure 9). *Langseth et al.* [1980] note that due to rapid sedimentation rates in the Aleutian Basin, especially over the last 10 Myr, the observed heat flow should be increased by 16–22% to correct for sedimentation. With this correction, the average heat flow is ~75 mW m^{-2}. In addition, the Aleutian back arc is composed of oceanic crust, in which radiogenic heat production is significantly less than that in continental crust. Thus, for comparison to continental back arcs in our compilation, the Aleutian heat flow should be further corrected upward by at least 10 mW m^{-2} to allow for differences in crustal radiogenic heat production. As radiogenic heat production in the Aleutian back arc is not well constrained, we do not include this latter correction.

[49] The Aleutian Basin heat flow is significantly higher than the expected ~45 mW m^{-2} heat flow for ~120 Ma oceanic crust [e.g., *Stein and Stein*, 1992]. There is some evidence for recent faulting in parts of the basin which might perturb the heat flow [*Cooper et al.*, 1992], but the spatial extent and apparent uniformity of the high heat flow seem to require a more widespread explanation. This conclusion is supported by seismic studies that indicate low P_n velocities of 7.8–8.0 km s^{-1} throughout the Aleutian Basin [*Levshin et al.*, 2001] and tomography data that indicates P wave velocities that are 1–2% slower than average mantle at 50–150 km depth [*Jin and Herrin*, 1980; *Bijwaard et al.*, 1998; *Bijwaard and Spakman*, 2000].

[50] The eastern Aleutian back arc and Alaska back arcs are composed of the Bering Shelf and Alaska mainland, respectively, which are both continental [*Fliedner and Klemperer*, 2000]. There are no surface heat flow data. However, seismic studies indicate that mantle velocities are anomalously low with P_n velocities of ~7.8 km s^{-1} beneath the Bering Sea shelf [*Fliedner and Klemperer*, 2000; *Levshin et al.*, 2001] and 7.8–8.0 km s^{-1} below continental Alaska [*Stone et al.*, 1987; *McNamara and Pasyanos*, 2002; *Levshin et al.*, 2001], suggesting shallow mantle temperatures of 650–900°C. Seismic tomography studies of this

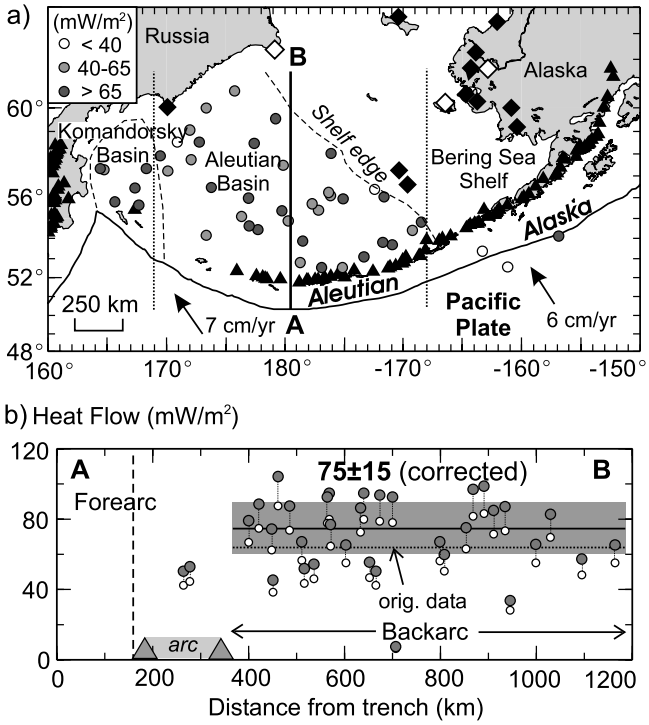

Figure 9. (a) Location map for the Aleutian and Alaska subduction zones. The diamonds indicate the volcanic fields of the Bering Sea basalt province; open diamonds are locations of mantle xenoliths [after *Akinin et al.*, 1997]. (b) Heat flow profile for the Aleutian back arc. The observed heat flow (open circles) has been corrected for the effects of sedimentation (solid circles) [*Langseth et al.*, 1980].

region indicate upper mantle (50–150 km depth) P wave velocities 1–3% slower than average mantle [*Estabrook et al.*, 1988; *Zhao et al.*, 1995; *Bijwaard et al.*, 1998; *Bijwaard and Spakman*, 2000], consistent with temperatures greater than 1150°C. In addition, throughout the Aleutian and Alaska subduction zone back arcs, there are at least 15 distinct basaltic volcanic fields younger than 10 Ma that form the Bering Sea basalt province [*Akinin et al.*, 1997] (Figure 9a). Upper mantle xenoliths from three fields indicate equilibrium temperatures of 850–1030°C at an estimated pressure of 1.5 GPa (~45 km) [*Akinin et al.*, 1997].

3.7. Kamchatka

[51] The Kamchatka subduction zone was established by at least 50 Ma [*Konstantinovskaia*, 2001]. Only diffuse small magnitude seismicity and GPS observations of little or no deformation suggest negligible present extension in the Kamchatka back arc [*Seno et al.*, 1996; *Takahashi et al.*, 1999]. The adjacent Kuril back arc (southernmost Sea of Okhotsk) was formed by spreading between 32 and 15 Ma [*Baranov et al.*, 2002], but this region of extension is more than 500 km southeast of our study area. In the Kamchatka back arc, the Sea of Okhotsk is characterized by high heat flow, 70 ± 18 mW m^{-2} (Figure 10) (*Sugrobov and Yanovsky* [1993], *Yamano* [1995], and data from http://www.heatflow.und.edu). Neither the effects of sedimentation on heat flow nor the amount of crustal radiogenic heat production are well constrained. Given that the crust is at least partially composed of oceanic material [*Konstantinovskaia*, 2001] with heat generation less than our reference value and that sediment thickness in the Sea of Okhotsk is >2 km [e.g., *Mooney et al.*, 1998], it is likely that the heat flow should be corrected upward for comparison to continental back arcs.

[52] P_n velocities are 7.8–7.9 km s^{-1} [*Levshin et al.*, 2001], suggesting uppermost mantle temperatures of 760–900°C. Tomography data at 50–120 km depth shows that, relative to average mantle velocities, P waves are generally 2% slow [*Bijwaard et al.*, 1998; *Gorbatov et al.*, 1999; *Bijwaard and Spakman*, 2000] and S waves are 4% to >7% slow [*Shapiro et al.*, 2000], consistent with upper mantle temperatures in excess of 1200°C. Slow mantle velocities are also observed in surface wave studies [e.g., *Kaila and Krishna*, 1984; *Ritzwoller and Levshin*, 1998]. In addition, the Kamchatka back-arc region is characterized by relatively low gravity, which has been modeled using a hot, low-density mantle [*Kogan*, 1975].

[53] The thermal structure of the northernmost Kamchatka back arc may be affected by the proximity of the edge of the subducting Pacific Plate, which could represent a region of complex mantle flow and unusual thermal conditions. However, mantle temperatures appear to be high well away from this boundary, and far from the region of Oligocene-Miocene extension in the Kuril back arc.

3.8. Northern Ryukyu-Korea

[54] The Korean Peninsula lies 450–750 km behind the northern Ryukyu subduction zone volcanic arc (Figure 11a). Although there is present extension in the East China Sea south of Korea and recent (30–12 Ma) extension in the Japan Sea to the northeast, the Korean Peninsula appears to be an intervening largely undeformed continental block [e.g., *Jolivet et al.*, 1994]. A heat flow profile shows the back-arc region has uniformly high heat flow that averages 69 ± 16 mW m^{-2} [*Yamano*, 1995] (Figure 11b). Radiogenic heat production is not well constrained. High upper mantle temperatures are supported by P_n velocities of 7.8–8.0 km s^{-1} [*Ritzwoller et al.*, 2002], suggesting Moho temperatures of 625–900°C. Tomography images show that upper mantle P wave velocities are ~2% slower than average upper mantle at 50–150 km depth [*Bijwaard et al.*, 1998; *Sadeghi et al.*, 2000; *Bijwaard and Spakman*, 2000], and surface wave velocities are low [*Ritzwoller and Levshin*, 1998], consistent with a hot upper mantle.

3.9. Sunda-Borneo

[55] The tectonics of the Sunda subduction zone and surrounding areas are relatively complex [*Hall and Morley*, 2004], but tectonic reconstructions, seismicity, and GPS observations indicate that neither the Sumatra nor Java segments of the Sunda margin have experienced significant recent back-arc extension [*Hamilton*, 1979; *Lee and Lawver*, 1995]. We focus our analysis on the Borneo region of the Sunda back arc (eastern Java). High heat flow is found at the volcanic arc and for over 800 km behind the arc, with an average value of 76 ± 18 mW m^{-1} (Figure 12) (data from http://www.heatflow.und.edu and *Hall and Morley* [2004]). The heat flow data primarily come from sedimentary basins where there has been rapid Neogene sedimentation [*Hall and Nichols*, 2002], which may decrease the surface heat

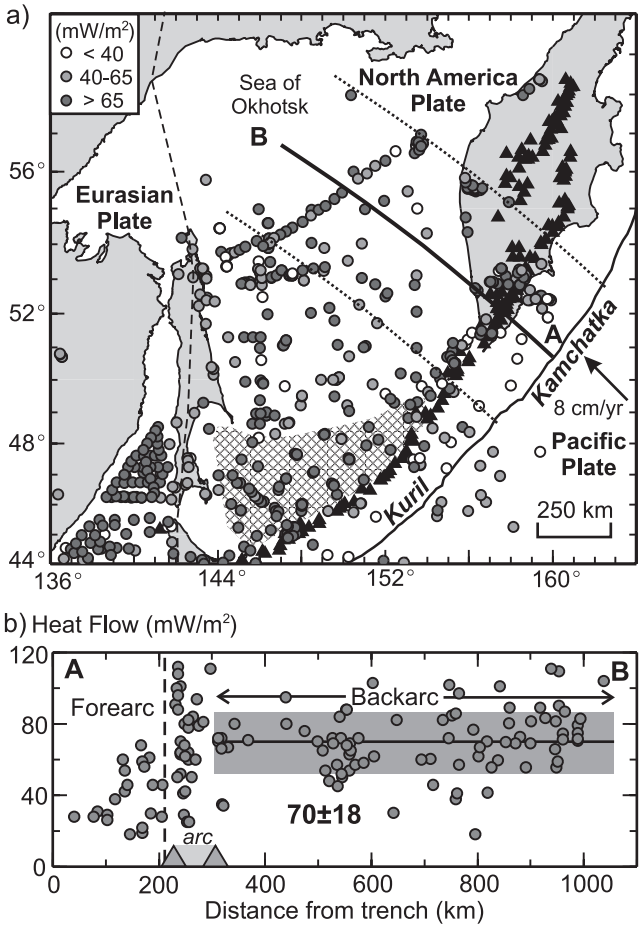

Figure 10. (a) Location map for the Kamchatka subduction zone. The hatched area is the region of Kuril back-arc extension. (b) Heat flow profile along line A-B.

flow. As neither the effects of sedimentation nor the crustal radiogenic heat production are well constrained, we have not introduced any corrections. Further evidence for high mantle temperatures comes from tomography studies that indicate P wave velocities that are ~2% slow [*Puspito and Shimazaki*, 1995; *Widiyantoro and van der Hilst*, 1997; *Bijwaard et al.*, 1998] and S wave velocities are ~4% slow [*Lebedev and Nolet*, 2003], relative to average mantle at ~100 km depth. These velocities are consistent with temperatures >1200°C in the shallow upper mantle.

[56] The high temperatures appear to extend well west of Borneo. Below the Sunda Shelf and Sumatra regions, upper mantle P wave velocities are ~2% slower than average upper mantle [*Puspito and Shimazaki*, 1995; *Widiyantoro and van der Hilst*, 1997; *Bijwaard et al.*, 1998] and S wave velocities are ~4% slower [*Lebedev and Nolet*, 2003]. This region is also characterized by high heat flow, >100 mW m^{-2} (data available at http://www.heatflow.und.edu), but factors that complicate the heat flow include recent folding and faulting in the sedimentary basins of Sumatra [*Tharmin*, 1985], enriched radiogenic heat production (up to 5 μW m^{-3}) in the granitoid basement rocks of the basins [*Gasparon and Varne*, 1995], and minor extension of the Sunda shelf between 30 and 40 Ma [*Lee and Lawver*, 1995; *Hall and Morley*, 2004]. Additional evidence for high temperatures are provided by sporadic Miocene-Quaternary basaltic volcanism throughout the Sunda back arc (including northern Borneo), and studies of gravity and basin subsidence history on the western Sunda shelf that indicate a thin elastic thickness [*Hall and Morley*, 2004 and references therein].

3.10. Other Regions

[57] There are a number of other back-arc areas that appear to be similarly hot to the back arcs discussed above, although extension and other tectonic processes may affect

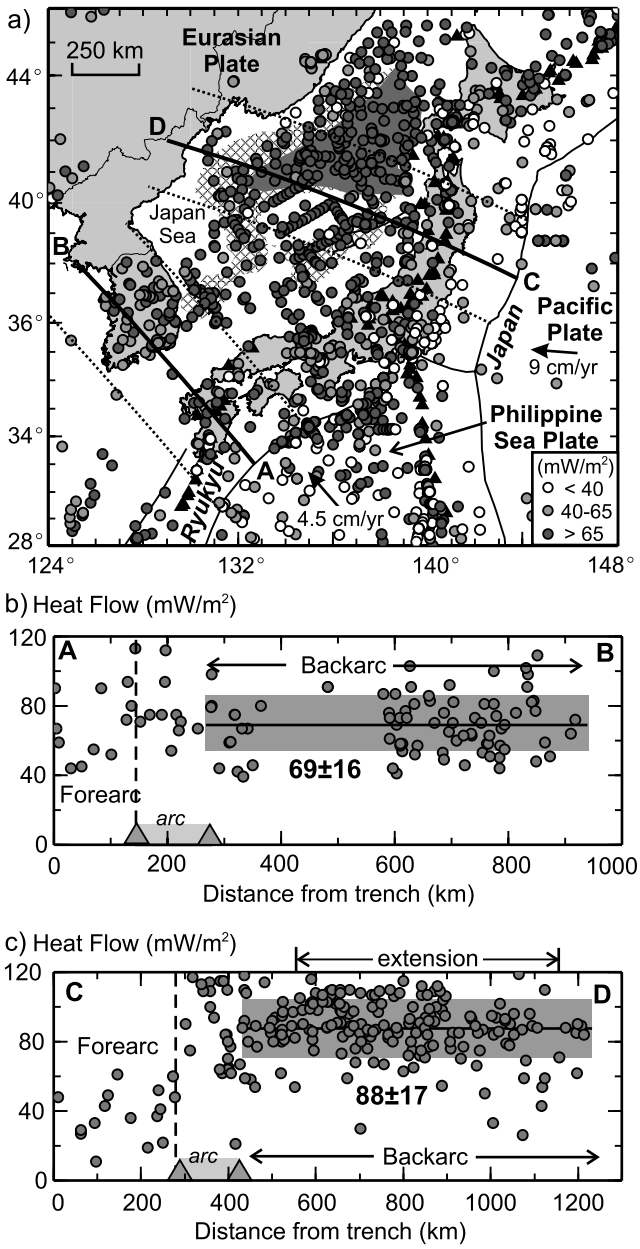

Figure 11. (a) Location map for the Japan and Ryukyu subduction zones. The hatched region shows the area with significant crustal extension and the dark shading is new oceanic crust created during Japan Sea opening (~12–30 Ma) [after *Jolivet et al.*, 1994]. (b) Heat flow profile (A-B) for Korean region of the Ryukyu subduction zone. (c) Heat flow profile (C-D) for the NE Japan subduction zone.

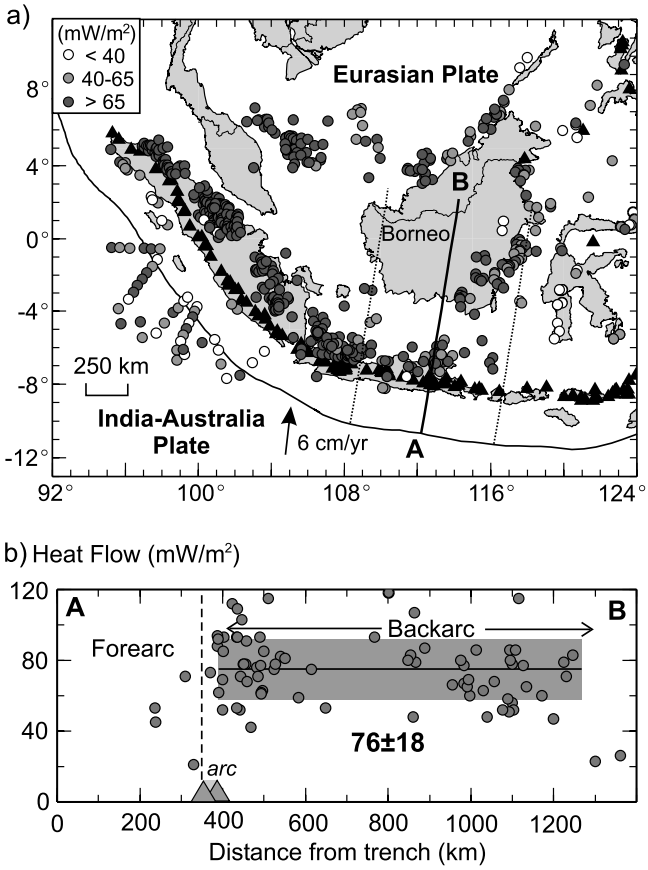

Figure 12. (a) Location map and (b) surface heat flow profile for the Sunda subduction zone.

the thermal structure, and some have only limited data that constrain mantle temperatures. Below, we summarize some of the published thermal constraints, but further work is necessary to better constrain the thermal regime of these regions.

3.10.1. Central America

[58] Central America and adjacent regions in the Caribbean Sea are unusual in that they form the back arc of two subduction zones, the Central America subduction zone on the west and the Lesser Antilles on the east. Simultaneous subduction has been ongoing for at least 85 Myr [*Meschede and Frisch*, 1998]. Although the region is complex in tectonics and structure, the thermal regime seems similar to other back arcs. Heat flow for the Caribbean Sea is 50–60 mW m^{-2} (*Epp et al.* [1970] and data from http://www.heatflow.und.edu), which is higher than expected for the ~90 Ma oceanic crust [*Meschede and Frisch*, 1998]. As this area is composed of oceanic crust with low radioactive heat generation, the measured heat flow should be corrected upward by ~10 mW m^{-2} for comparison with the continental back arcs in our study. High temperatures are also suggested by shear wave velocities up to 4% slower than average mantle at 50 to 150 km depth throughout Central America [*Grand*, 1994; *van der Lee and Nolet*, 1997; *Goes and van der Lee*, 2002]. The thermal regime of this area may be affected by a slab window associated with subduction of the Cocos-Nazca spreading ridge near 10°N [*Johnston and Thorkelson*, 1997], although it is difficult to explain the regionally high temperatures with this mechanism alone.

3.10.2. Southern Europe and Asia

[59] The recent tectonics of southern Europe and Asia are highly complex, and there are a number of back arcs that are currently undergoing extension. Nevertheless, it is useful to point out the evidence for high back-arc temperatures. Surface heat flow in southern Europe is generally high (>60 mW m^{-2}, with heat flow >100 mW m^{-2} in some regions) (*Cermak and Rybach* [1979], *Cermak* [1993], and data from http://www.heatflow.und.edu). Although there are fewer heat flow measurements in southern Asia, the back-arc regions of the subduction/collision margin are also characterized by high heat flow (*Artemieva and Mooney* [2001] and data from http://www.heatflow.und.edu). Inferred temperatures at 50 km depth are >1000°C [*Artemieva and Mooney*, 2001]. In addition, both southern Europe and Asia are characterized by low upper mantle seismic velocities from surface wave tomography and P_n velocity studies [*Ritzwoller and Levshin*, 1998; *Ritzwoller et al.*, 2002]. Tomography images using P and S waves for southern Europe show low velocities at 50 to 150 km depth, with velocities more than 5% slower than average mantle, suggesting temperatures greater than 1000°C at 50 km depth [*Goes et al.*, 2000]. We propose that the generally high temperatures beneath southern Europe and adjacent Asia are because they are in current or recent back arcs.

3.10.3. Eastern Australia

[60] Numerous observations suggest that the Phanerozoic lithosphere of eastern Australia is hot. Surface heat flow is generally greater than 70 mW m^{-2} (*Cull* [1991] and data from http://www.heatflow.und.edu). Seismic tomography studies show that S wave velocities are 2–3% slower than average mantle velocities at depths of 80–170 km [e.g., *Simons et al.*, 1999]. From seismic tomography data, *Goes et al.* [2005] infer temperatures greater than 1000°C at 80 km depth, consistent with P-T estimates of mantle xenoliths for this area [*O'Reilly et al.*, 1997]. This region is also characterized by sporadic Cenozoic basaltic volcanic centers. Currently, the subduction margin is over 1000 km east of the eastern coast of Australia. However, prior to the initiation of Tasman Sea opening at ~90 Ma, the subduction margin approximately coincided with the Australian east coast [e.g., *Gaina et al.*, 1998]. We suggest that the present-day high temperatures throughout eastern Australia may be associated with the long history of adjacent subduction, but a more detailed study is necessary to better constrain the thermal effects of the opening of the Tasman Sea.

3.10.4. Japan Sea: Example of a Back Arc With Local Extension

[61] In our compilation, we have avoided back arcs with significant recent extension or spreading that may perturb the thermal regime. A full examination of the thermal effects of extension and back-arc spreading is beyond the scope of the current study. However, we note that all well-studied extensional back arcs exhibit characteristics similar to those described in our compilation (e.g., high heat flow and low mantle seismic velocities). It is also important to recognize that in order to initiate extension in the back arc, the lithosphere must be sufficiently weak to deform under available plate tectonic forces; high back-arc temperatures prior to extension provide a weakening mechanism.

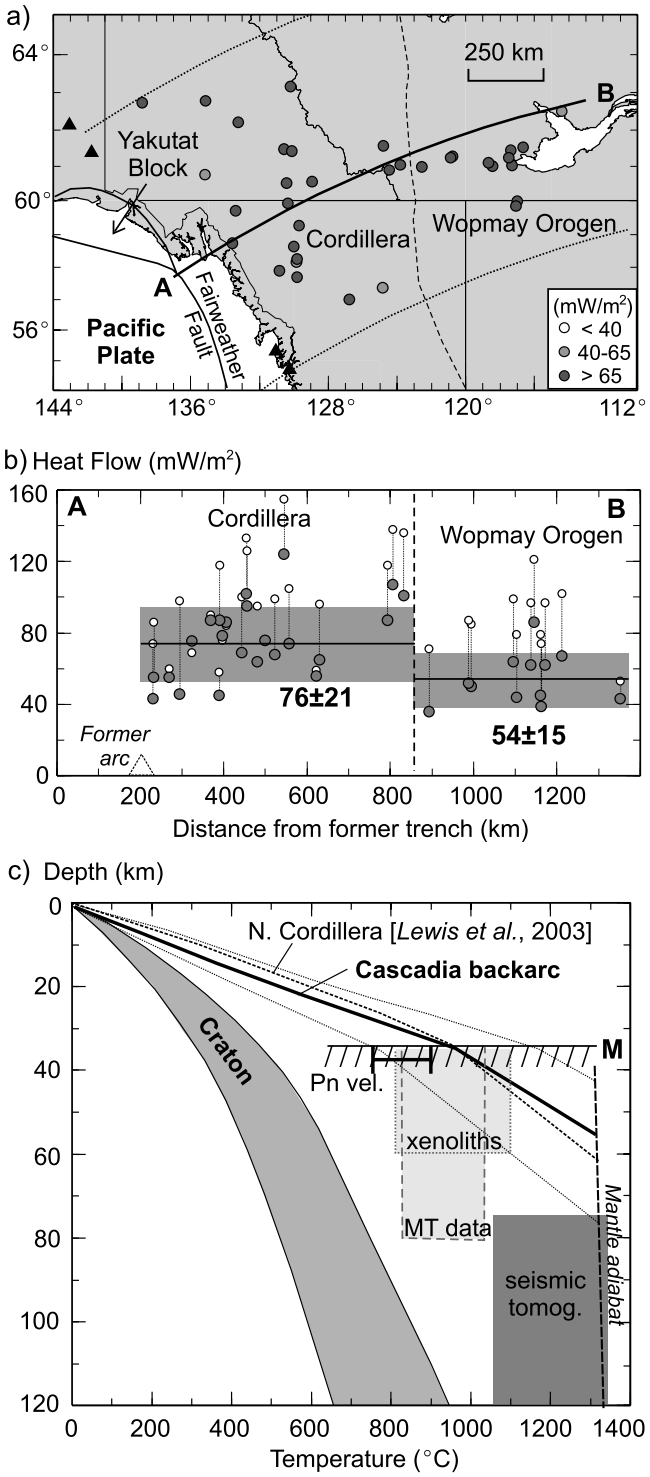

Figure 13. (a) Heat flow data for the Northern Canadian Cordillera. Subduction along this margin ceased at ~42 Ma. (b) Heat flow profile. The original heat flow values (open circles) have been corrected for variations in upper crustal heat production (solid circles) (see text). (c) Observational constraints on thermal structure. The dashed line is the geotherm from *Lewis et al.* [2003]. The Cascadia back arc and Archean craton geotherms are shown for comparison.

[62] As an example, we summarize observations for the back-arc Japan Sea. The basement of the Japan Sea is composed of both highly extended continental crust and oceanic crust formed during Japan Sea opening between 30 and 12 Ma [*Jolivet et al.*, 1994]. A profile across the NE Japan subduction zone shows high heat flow, 88 ± 17 mW m^{-2} (Figure 11c) [*Yamano*, 1995]. The heat flow data have not been corrected for the effects of sedimentation nor differences in crustal radiogenic heat production between oceanic and continental basement. This heat flow is similar to that expected for ~20 Myr old oceanic crust [e.g., *Stein and Stein*, 1992]. However, new oceanic crust is confined to only a small part of the back arc, and as noted by previous authors [e.g., *Watanabe et al.*, 1977], the heat flow for the Japan Sea is remarkably uniform, despite heterogeneities in the amount of extension and the creation of small regions of oceanic crust.

[63] Other indicators of regionally high temperatures are (1) P wave velocities 2–6% slower than average mantle at ~100 km depth throughout the Japan Sea [*Bijwaard and Spakman.*, 2000; *Zhao*, 2001, and references therein]; (2) anomalously low P and S wave velocities in the uppermost mantle from surface wave tomography [*Ritzwoller and Levshin*, 1998]; (3) regionally high seismic attenuation to depths of at least 200 km [*Flanagan and Wiens*, 1994; *Nakajima and Hasegawa*, 2003]; (4) upper mantle xenoliths from the eastern coast of Honshu (NE Japan) that indicate temperatures of ~1000°C at 40 km depth [*Nakajima and Hasegawa*, 2003, and references therein]; and (5) the presence of Neogene to Quaternary basalt fields on the northeastern China coast, west of the region of Japan Sea extension.

[64] These observations suggest that shallow mantle temperatures beneath the Japan Sea are comparable to those of the northern Cascadia back arc (e.g., Figure 4c). Other extensional back arcs, including the Kuril and Tonga back arcs, exhibit similar evidence of widespread high temperatures in the uppermost mantle [e.g., *Barazangi et al.*, 1975; *Watanabe et al.*, 1977; *Flanagan and Wiens*, 1994; *Zhao*, 2001; *Wiens and Smith*, 2003]. In their compilation of heat flow observations, *Watanabe et al.* [1977] found that heat flow values in western Pacific back-arc basins were generally larger than expected for the age of the back-arc crust and suggested an additional heat source may be shallow small-scale back-arc mantle convection. However, other studies have argued that with improved constraints on back-arc crustal age and a reanalysis of the heat flow data, the discrepancy may not be significant [e.g., *Anderson*, 1980]. A detailed study of the thermal structure of extensional back arcs and accurate thermal modeling of crustal extension is required to determine if an additional mantle heat source is needed to satisfy the heat budget of these regions.

4. Former Back Arcs

[65] Although our compilation focuses on present-day subduction zones, it is also important to consider the thermal regime of regions that are in the back-arc areas of recent subduction zones. The decrease in temperatures with time after termination of subduction may constrain the processes controlling the thermal structure. In this section,

we provide initial information through an overview of observational constraints on upper mantle temperatures at two former continental back arcs.

4.1. Northern Canadian Cordillera (~42 Ma)

[66] Prior to the Eocene, the northern Canadian Cordillera was the back arc for Farallon/Kula Plate subduction below the North America Plate. Plate reconstructions suggest that the subduction margin was cut off by the Queen Charlotte transform fault at ~42 Ma [*Engebretson et al.*, 1985]. High surface heat flow across the northern Cordillera is partially attributed to enhanced upper crustal radiogenic heat production, which averages over 4 $\mu W\ m^{-3}$ north of 60°N (*Lewis et al.* [2003] and additional measurements by T. Lewis, as reported by *Flück* [2003]) (Figure 13). Corrected to a common heat generation of 1.3 $\mu W\ m^{-3}$, the heat flow for the northern Cordillera is 76±21 mW m^{-2}. Geotherms calculated from heat flow–heat generation data indicate temperatures at the Moho (33–36 km depth) of 850–950°C [*Lewis et al.*, 2003], similar to the present-day Cascadia back arc (Figure 13c). The eastern limit of the high heat flow is the Wopmay Orogen, a stable Proterozoic continental block.

[67] Seismic refraction studies indicate P_n velocities of 7.8–7.9 km s^{-1} [*Clowes et al.*, 2005], consistent with Moho temperatures of 760–900°C. Tomography studies show that, relative to average mantle velocities at ~100 km depth, P wave velocities are 1–2% slow [*Frederiksen et al.*, 2001] and S wave velocities are 3–4% slow [*Grand*, 1994; *Frederiksen et al.*, 1998; *van der Lee and Frederiksen*, 2005] (Figure 5a), suggesting mantle temperatures greater than 1100°C. The effective elastic thickness for the northern Cordillera is generally less than 20 km, indicating high temperatures (Figure 5b) [*Flück et al.*, 2003]. Surface elevations across the Cordillera are 1–2 km, although the crust is only 33–36 km thick, consistent with a hot, low-density upper mantle [*Lewis et al.*, 2003]. There is widespread Tertiary and Quaternary basaltic volcanism throughout this region and P-T estimates from upper mantle xenoliths for this area yield temperatures between 805 and 1100°C [*Harder and Russell*, 2006]. It was assumed that the lowest temperature (805°C) corresponds to the temperature just below the Moho. Electrical conductivity data yield similar temperature estimates of 820–1020°C at depths of 35–80 km [*Ledo and Jones*, 2005]. Taken together, these observations indicate that the thermal structure of the northern Canadian Cordillera is similar to that of the northern Cascadia back arc. It has been proposed that the high temperatures for the northern Cordillera are related to back-arc mantle flow associated with past subduction [*Lewis et al.*, 2003]. We conclude that the thermal effects of subduction-related back-arc mantle dynamics persist, with little decay, for over 40 Myr after subduction termination.

4.2. Appalachians (~260 Ma)

[68] The Appalachian mountains in eastern North America represent an orogenic belt developed by the accretion of arcs and microcontinents to the North America craton [e.g., *Hatcher*, 1989; *Keller and Hatcher*, 1999]. The Appalachian region is the former back arc of primarily westward directed subduction between 500 and 260 Ma. The last major deformation was the Alleghanian Orogeny (325–260 Ma).

[69] The Appalachian surface heat flow is 50–60 mW m^{-2} [*Jaupart et al.*, 1982; *Jaupart and Mareschal*, 1999], which is slightly higher than that of the adjacent North American craton (42–10 mW m^{-2}). Much of the difference in heat flow can be explained by higher radiogenic heat production in the Appalachian crust [*Jaupart et al.*, 1982; *Jaupart and Mareschal*, 1999], although *Artemieva and Mooney* [2001] suggest that there may be higher temperatures at depth and a thinner thermal lithosphere below the Appalachians, due to a higher mantle heat flow. They determine a temperature of 700–800°C at 50 km depth for the Appalachians, compared to 500–600°C for the craton.

[70] In seismic tomography images, the Appalachian region mantle is characterized by only a small S wave velocity anomaly (generally <1%), relative to average mantle velocities at 50–150 km depth [*Grand*, 1994; *van der Lee and Nolet*, 1997; *Goes and van der Lee*, 2002]. In contrast, S wave velocities below the Archean North America craton are 3–4% faster than average mantle velocities, which may reflect 100–300°C higher temperatures below the Appalachian region [*Goes and van der Lee*, 2002]. Overall, it appears that the thermal structure of the Appalachian region is only slightly hotter than the adjacent Archean craton. If the excess heat comes from back-arc mantle processes associated with past subduction, this suggests that much of the back-arc thermal anomaly decays within 300 Myr of subduction termination.

5. Constraints on Back-Arc Mantle Dynamics

[71] In our compilation of thermal constraints for back arcs that have not experienced recent extension or that have flat slabs, we find that all exhibit characteristics indicative of high temperatures in the uppermost mantle, including high surface heat flow, low mantle seismic velocity, high mantle temperatures from xenoliths, and basaltic volcanism (Table 1). It is well recognized that back arcs that have undergone recent extension are hot [e.g., *Watanabe et al.*, 1977; *Wiens and Smith*, 2003]. In these areas, the high back-arc temperatures have generally been attributed to extension. It has not been widely appreciated that back arcs with no thermally significant extension are similarly hot. Where high back-arc temperatures have been previously recognized, they have usually been explained with site-specific factors, such as the proximity of a slab window or slab edge (southernmost South America and Kamchatka), thickened continental crust enriched in radiogenic elements (central Andes), or anomalous mantle upwelling (Cascadia). Although these factors may explain high temperatures at one or several subduction zones, observations of high temperatures for nearly all back arcs that we have examined suggests that there may be a common subduction-related mechanism.

[72] Most studies of mantle wedge thermal structure have focused on the volcanic arc region, where temperatures greater than 1200°C are required for magma generation. High subarc mantle temperatures are usually assumed to be produced by mantle flow that carries heat from greater depths into the wedge corner. Recognition of uniformly

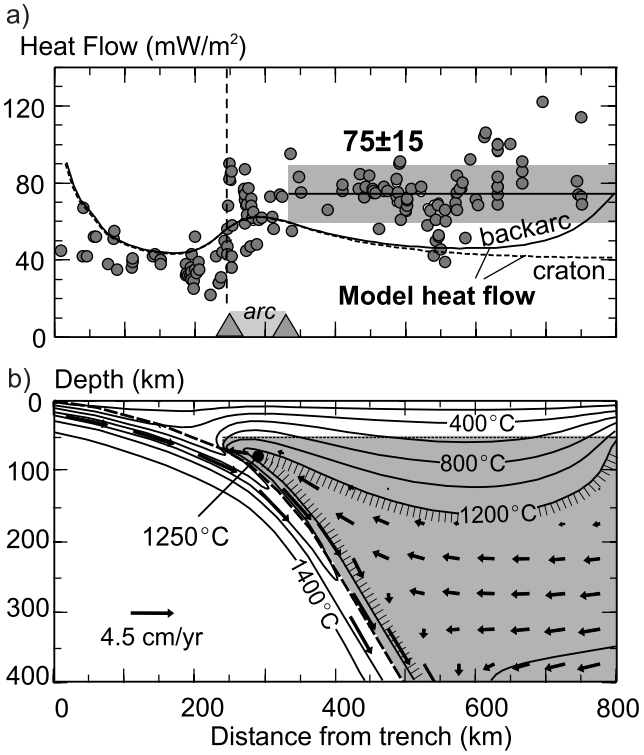

Figure 14. (a) Modeled surface heat flow (solid line) and (b) thermal model of slab-driven corner flow for the Cascadia subduction zone [after *Currie et al.*, 2004]. The mantle wedge (grey region in Figure 14b) has a wet olivine dislocation creep rheology. On the landward boundary, the inferred Cascadia back-arc geotherm (as in Figure 4c) is prescribed. The focusing of flow into the wedge corner by the temperature-dependent mantle rheology results in low back-arc lithosphere temperatures and heat flow, inconsistent with observations. The dashed line in Figure 14a shows the predicted heat flow for a model in which an Archean craton geotherm is prescribed to the landward boundary.

high back-arc mantle temperatures and thin lithosphere for hundreds of kilometers behind the volcanic arc places important and very restrictive constraints on the back-arc mantle flow regime:

[73] 1. A large amount of heat must be fed into the back arc, probably from the deeper global convective system, to balance the heat lost to the cold slab, arc volcanics, high back-arc heat flow, and slab dehydration reactions. A shallow heat source immediately landward of the back arc is not likely, especially for back arcs that are adjacent to cold Archean cratons, such as Cascadia and South America. Mantle flow in the back arc must tap this large heat source and carry the heat upward into the shallow back-arc mantle and mantle wedge corner.

[74] 2. The deep heat source and back-arc mantle flow must be maintained over tens to hundreds of million years for some subduction zones. The thermal constraints in our study cover a range of timescales. Mantle seismic velocities reflect the present temperatures. Surface heat flow reflects the upper mantle thermal structure on timescales of 50–100 Myr, the thermal time constant for the lithosphere. Mantle xenolith temperatures represent the conditions at the time of their chemical equilibration, and back-arc volcanics reflect the thermal regime at the time of extrusion. The agreement in temperatures from all observations suggests that a long-lived process, not a short-term transient phenomenon, maintains the high back-arc mantle temperatures.

[75] 3. There must be only a small dependence of the back-arc thermal regime on subduction parameters, such as the age of subducting plate and subduction rate. Surface heat flow, mantle seismic velocities and other observations suggest very similar mantle temperatures for all the back arcs that we have examined, which range from those with a young oceanic plate and low subduction velocity (e.g., northern Cascadia, 8 Ma, 4.5 cm yr^{-1}) to those with an old plate and high rate of subduction (e.g., Kamchatka, 90 Ma, 8 cm yr^{-1}).

[76] Flow in the back-arc mantle is probably driven both by thermal buoyancy forces and by viscous coupling between the subducting slab and overlying mantle (corner flow). In slab-driven corner flow mantle wedge material is carried downward with the subducting slab, producing a return flow that carries hot material from depth upward and toward the volcanic arc. Numerical models of corner flow show that the temperature-dependent mantle rheology produces a strong focusing of flow into the wedge corner, enhancing temperatures below the arc (Figure 14). However, this flow regime produces a stagnant region farther landward in the shallow back-arc mantle, resulting in cool temperatures and low surface heat flow, inconsistent with observations [*Currie et al.*, 2004]. To maintain uniformly high mantle temperatures over back-arc widths of hundreds of kilometers, some form of vigorous thermally driven convection in the back-arc mantle appears to be required. Whereas the velocity of slab-driven corner flow is limited by the subduction rate, thermal convection can occur at much faster velocities, providing more efficient transfer of heat from the deeper mantle into the back arc.

[77] For vigorous thermal convection to be the dominant flow regime in the back-arc mantle, the mantle viscosity must be low [e.g., *Ida*, 1983; *Honda et al.*, 2002]. Laboratory data show that even a small amount of water significantly reduces the effective viscosity of olivine and other upper mantle minerals [e.g., *Hirth and Kohlstedt*, 1996]. At a subduction zone, dehydration reactions in the subducting slab release significant amounts of water to the overlying mantle [e.g., *Peacock*, 1993]. Therefore it is expected that the mantle above the subducting slab should incorporate substantial amounts of water and thus be much weaker than normal drier mantle.

[78] Several recent modeling studies have examined the effects of hydration and low viscosity on the back-arc convective system. *Honda et al.* [2002], *Honda and Saito* [2003], and *Honda and Yoshida* [2005] showed that a low-viscosity zone above the subducting slab will promote small-scale convection, which may explain observed lateral variations in seismic velocity and the along-margin distribution of arc volcanism. Models by *Arcay et al.* [2005, 2006] also indicate that the low viscosities associated with the addition of water can enhance convection above a subducting plate, producing high mantle wedge temperatures and the thinning of the overriding lithosphere. These studies have focused on the volcanic arc region, as the majority of slab dehydration is believed to occur at shallow

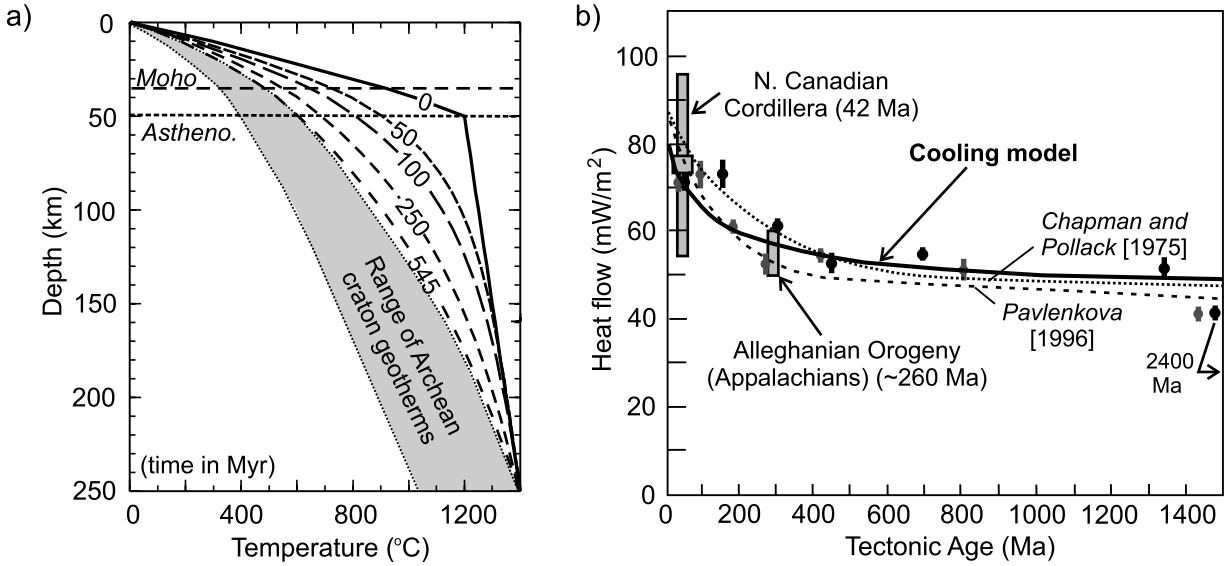

Figure 15. (a) Thermal evolution of the back-arc cooling model. The zero time corresponds to the termination of vigorous back-arc convection and onset of conductive cooling. (b) Heat flow versus tectonic age for the cooling model (solid line). Grey bars are the observed heat flow for the Northern Canadian Cordillera and Appalachians (former back arcs). Also shown is the proposed cooling trend from studies of the decay in heat flow with thermotectonic age for different orogenies (dotted and dashed lines). The circles are the data used in these studies (bars show the uncertainty range).

depths (<150 km). Our compilation shows that high temperatures and thin lithosphere occur well behind the volcanic arc. We suggest that water may be efficiently mixed through the back arc by both slab-driven and thermally driven convection. This should be examined in future modeling studies.

[79] Some indication for the existence of a broad, low-viscosity back arc at a number of subduction zones comes from independent observations of the Earth's surface response to transient crustal loads, for example, postglacial rebound [e.g., *James et al.*, 2000; *Ivins and James*, 1999], postseismic relaxation [e.g., *Wang*, 2006, and references therein], and lacustrine loading/unloading [e.g., *Bills et al.*, 1994; *Okuno and Nakada*, 1998]. These studies indicate that low mantle viscosities of $\sim 10^{19}$ Pa s are found well behind the volcanic arc for a number of subduction zones, including Cascadia, southernmost South America, and Japan. Furthermore, studies of dynamic topography of the Tonga subduction zone back arc show that a ~800 km wide region with a viscosity at least a factor of 10 less than the surrounding mantle provides the best fit to surface topography, geoid and gravity observations [*Billen and Gurnis*, 2001; *Billen et al.*, 2003]. In addition, in the western United States (former back arc), *Dixon et al.* [2004] argue that the observed low viscosities and low shear wave velocities require the presence of dissolved water in the upper mantle, as well as temperatures close to the wet mantle solidus over distances of more than 800 km from the former subduction margin.

[80] In our conceptual model, we propose that the back-arc mantle convective system is dominated by vigorous thermal convection, resulting from a viscosity reduction by volatiles associated with subducting slab dehydration. The rapidly overturning convection cells will produce an overall hot thermal structure, but with short-wavelength temperature variations of hundreds of degrees. In our study, we have focused on the large-scale indicators of thermal structure. We note that recent high-resolution seismic studies in the western United States have identified short-wavelength (~100 km) velocity variations that have been interpreted to represent temperature variations associated with small-scale convection [e.g., *Gao et al.*, 2004; *Forsyth and Yang*, 2005]. Similar high-resolution studies of the back-arc regions that we have examined may place stronger constraints on the details of the back-arc convective system.

6. Decay in Back-Arc Temperatures With Time

[81] The vigorous convection model provides a mechanism for carrying a large amount of heat into the back-arc mantle. The high back-arc temperatures may persist for a long time after subduction has ceased. *Hyndman et al.* [2005] proposed that continental mobile belts are located in former back-arc regions, where the preexisting hot, weak lithosphere facilitates deformation and shortening, i.e., the vise or inherited weakness model [e.g., *Ellis et al.*, 1998].

[82] A critical question for continental tectonics is the nature of the decay in back-arc temperatures after the termination of subduction. In our conceptual model, the decline in back-arc temperatures with time following subduction termination is related to the decay in vigorous back-arc mantle convection, which in turn depends on how long slab dehydration continues after subduction termination, the dynamics of the subducting slab (i.e., does slab break-off occur?), and how quickly water is lost from the back-arc mantle through upward diffusion and partitioning into arc and back-arc magmas. Although vigorous convection may persist for a few tens of million years after subduction termination [e.g., *Dixon et al.*, 2004], we have examined the

first-order approximation that there is abrupt termination of convection, followed by conductive cooling of the back-arc lithosphere.

[83] In our simple one-dimensional conductive model, the initial thermal structure is assumed to be that of a hot back arc, with a surface heat flow of 80 mW m^{-2}, a temperature of 1200°C at 50 km depth (taken to be the base of the back-arc lithosphere), and a linear, approximately adiabatic, temperature increase to 1400°C at 250 km depth (Figure 15a). The continental crust is 35 km thick, with a thermal conductivity of 2.5 W m^{-1} K^{-1} and heat production of 1.3 and 0.4 μW m^{-3} in the 10 km upper and 25 km lower crust, respectively. The mantle has a thermal conductivity of 3.1 W m^{-1} K^{-1} and heat production of 0.02 μW m^{-3}.

[84] The model is allowed to cool conductively, keeping the upper and lower boundaries fixed at 0°C and 1400°C, respectively. This model is similar to a cooling oceanic plate model [e.g., *Stein and Stein*, 1992]. A plate thickness of 250 km is based on the average lithosphere thickness for older stable platforms and cratons [e.g., *Jaupart and Mareschal*, 1999]. An alternative model would be to take the base of the model at the 410 km phase boundary, where temperatures are ~1450°C from olivine-spinel phase transition data [e.g., *Thompson*, 1992, and references therein]. However, there is little difference in temperatures or heat flow in either case compared to a half-space cooling model for ages less than 200–300 Myr.

[85] The evolution of the thermal regime and surface heat flow are shown in Figure 15. The most rapid cooling occurs in the first 50–100 Myr. After ~300 Myr, much of the back-arc heat has dissipated. The modeled thermal structure and heat flow is in good agreement with those for the Northern Canadian Cordillera and Appalachian former back arcs. The simple model can also be compared to the observed heat flow for Phanerozoic orogenic belts [e.g., *Chapman and Pollack*, 1975; *Pavlenkova*, 1996] (Figure 15b). The age of the orogenic belts is given by their thermotectonic age, which reflects the time of peak regional metamorphism or plutonism; this age may be a few tens of million years after subduction termination. To first-order, the simple conductive cooling model fits the observed heat flow, suggesting that times of subduction termination, cessation of vigorous convection and thermotectonic age are similar (i.e., within a few 10 Myr).

7. Conclusions

[86] A remarkable feature of subduction zones is that the arc and back-arc regions are extremely hot, despite the cooling effects of the subducting plate. It is well established that the presence of an active volcanic arc at most subduction zones requires high temperatures (>1200°C) in the mantle wedge below the arc for magma generation. However, it has not been widely recognized that high temperatures in the upper mantle extend for hundreds of kilometers behind the volcanic arc, even in back arcs that have not undergone recent extension. In our compilation of observational constraints on the thermal structure, we find that nearly all nonextensional back arcs share similar characteristics: (1) surface heat flow of >70 mW m^{-2} for continental crust with average radiogenic heat production (>60 mW m^{-2} for oceanic crust with much lower heat production), (2) P_n velocities of <8.0 km s^{-1} for the most common back-arc crustal thickness of ~35 km, (3) slow upper mantle seismic velocities from tomography studies, with P waves generally 1–3% slow and S waves >3% slow, relative to average mantle velocities at 50–150 km depth, (4) effective elastic thickness of <30 km, (5) estimates of high in situ temperatures in the shallow back-arc mantle from peridotite xenoliths, (6) widespread sporadic basaltic volcanism, and (7) high elevations (1–2 km) for back-arc continental crustal thicknesses of ~35 km, higher elevations in areas of thickened crust.

[87] Taken together, these observations are consistent with uniformly high temperatures in the shallow back-arc mantle over back-arc widths that, in some areas, extend to more than 900 km. Estimated temperatures are 800–1000°C at ~35 km depth (i.e., the Moho for most continental back arcs) and a lithosphere thickness, defined by a temperature of about 1200°C, of 50–60 km. Back arcs that are currently extending or have experienced recent extension (e.g., the U.S. Basin and Range and the Japan Sea) appear to be similarly hot, but further work is necessary to separate the effects of extension from the underlying thermal structure associated with subduction. The only evidence that any back arc is cool comes from regions where there is a very flat subducting slab, such as the Peru region of South America. In these areas, there may be little or no convecting asthenosphere between the slab and overlying crust.

[88] We propose that high temperatures in the shallow back-arc mantle are a characteristic feature of subduction zones, related to shallow back-arc mantle flow associated with subduction. The source of heat is probably the deeper high temperatures maintained by general mantle circulation not related to subduction. Vigorous thermal convection in the back-arc mantle must efficiently carry this heat into the subduction zone region, resulting in the observed uniformly high back-arc temperatures. Widespread vigorous shallow convection may be promoted by water released from the subducting slab. This model has important consequences of uniformly thin, hot, and weak back-arc lithospheres. Following termination of subduction, the decay of high back-arc temperatures and establishment of a strong lithosphere occur over a timescale of about 300 Myr.

[89] **Acknowledgments.** Stimulating discussions with Kelin Wang and Stephane Mazzotti and thoughtful reviews by Saskia Goes, Mihai Ducea, and Tim Dixon allowed us to clarify our ideas and improved the manuscript. We thank Saskia Goes for the seismic velocity-temperature conversion data used in this study and Andrew Frederiksen for the seismic tomography data in Figure 5a. This is a Geological Survey of Canada contribution.

References

Akinin, V. V., M. F. Roden, D. Francis, J. Apt, and E. Moll-Stalcup (1997), Compositional and thermal state of the upper mantle beneath the Bering Sea basalt province: Evidence from the Chukchi Peninsula of Russia, *Can. J. Earth Sci.*, *34*, 789–800.

Allmendinger, R. W., R. E. Jordan, S. M. Kay, and B. L. Isacks (1997), The evolution of the Altiplano-Puna Plateau of the central Andes, *Annu. Rev. Earth Planet. Sci.*, *25*, 139–174.

Anderson, R. N. (1980), 1980 update of heat flow in the East and Southeast Asian Seas, in *The Tectonic and Geologic Evolution of Southeast Asian Seas and Islands*, *Geophys. Monogr. Ser.*, vol. 23, edited by D. E. Hayes, pp. 319–326, AGU, Washington, D. C.

Andrews, D. J., and N. H. Sleep (1974), Numerical modelling of tectonic flow behind island arcs, *Geophys. J. R. Astron. Soc.*, *38*, 237–251.

Arcay, D., E. Tric, and M.-P. Doin (2005), Numerical simulations of subduction zones: Effect of slab dehydration on the mantle wedge dynamics, *Earth Planet. Sci. Lett.*, *149*, 133–153.

Arcay, D., M.-P. Doin, E. Tric, R. Bousquet, and C. de Capitani (2006), Overriding plate thinning in subduction zones: Localized convection induced by slab dehydration, *Geochem. Geophys. Geosyst.*, *7*, Q02007, doi:10.1029/2005GC001061.

Artemieva, I. M., and W. D. Mooney (2001), Thermal thickness and evolution of Precambrian lithosphere: A global study, *J. Geophys. Res.*, *106*, 16,387–16,414.

Babeyko, A. Y., V. V. Sobolev, R. B. Trumbull, O. Oncken, and L. L. Lavier (2002), Numerical models of crustal scale convection and partial melting beneath the Altiplano-Puna plateau, *Earth Planet. Sci. Lett.*, *199*, 373–388.

Baranov, B., H. K. Wong, K. Dozorova, B. Karp, T. Ludmann, and V. Karnaukh (2002), Opening geometry of the Kurile Basin (Okhotsk Sea) as inferred from structural data, *Island Arc*, *11*, 206–219.

Barazangi, M., W. Pennington, and B. Isacks (1975), Global study of seismic wave attenuation in the upper mantle behind island arcs using pP waves, *J. Geophys. Res.*, *80*, 1079–1092.

Baumont, D., A. Paul, G. Zandt, and S. L. Beck (2001), Inversion of Pn travel times for lateral variations of Moho geometry beneath the central Andes and comparison with the receiver functions, *Geophys. Res. Lett.*, *28*, 1663–1666.

Baumont, D., A. Paul, G. Zandt, S. L. Beck, and H. Pedersen (2002), Lithospheric structure of the central Andes based on surface wave dispersion, *J. Geophys. Res.*, *107*(B12), 2371, doi:10.1029/2001JB000345.

Bijwaard, H., and W. Spakman (2000), Non-linear global P-wave tomography by iterated linearized inversion, *Geophys. J. Int.*, *141*, 71–82.

Bijwaard, H., W. Spakman, and E. R. Engdahl (1998), Closing the gap between regional and global travel time tomography, *J. Geophys. Res.*, *103*, 30,055–30,078.

Billen, M. I., and M. Gurnis (2001), A low viscosity wedge in subduction zones, *Earth Planet. Sci. Lett.*, *193*, 227–236.

Billen, M. I., M. Gurnis, and M. Simons (2003), Multiscale dynamics of the Tonga-Kermadec subduction zone, *Geophys. J. Int.*, *153*, 359–388.

Bills, B. G., D. R. Currey, and G. A. Marshall (1994), Viscosity estimates for the crust and upper mantle from patterns of lacustrine shoreline deformation in the eastern Great Basin, *J. Geophys. Res.*, *99*, 22,059–22,086.

Black, P. R., and L. W. Braile (1982), P_n velocity and cooling of the continental lithosphere, *J. Geophys. Res.*, *87*, 10,557–10,568.

Blackwell, D. D. (1969), Heat flow in the northwestern United States, *J. Geophys. Res.*, *74*, 992–1077.

Blackwell, D. D. (1978), Heat flow and energy loss in the western United States, in *Cenozoic Tectonics and Regional Geophysics of the Western Cordillera*, edited by R. B. Smith and G. P. Eaton, *Geol. Soc. Am. Mem.*, *152*, 175–208.

Blackwell, D. D., and M. Richards (2004), Geothermal map of North America, scale 1:6,500,000, Am. Assoc. of Pet. Geol., Tulsa, Okla.

Blackwell, D. D., J. L. Steele, M. K. Frohme, C. F. Murphey, G. R. Priest, and G. L. Black (1990a), Heat flow in the Oregon Cascade Range and its correlation with regional gravity, Curie point depths and geology, *J. Geophys. Res.*, *95*, 19,475–19,493.

Blackwell, D. D., J. L. Steele, S. Kelley, and M. A. Korosec (1990b), Heat flow in the state of Washington and thermal conditions in the Cascade Range, *J. Geophys. Res.*, *95*, 19,495–19,516.

Burianyk, M. J. A., and E. R. Kanasewich (1995), Crustal structure of the Omineca and Intermontane belts, southeastern Canadian Cordillera, *J. Geophys. Res.*, *100*, 15,303–15,316.

Burianyk, M. J. A., E. R. Kanasewich, and N. Udey (1997), Broadside wide-angle seismic studies and three-dimensional structure of the crust in the southeast Canadian Cordillera, *Can. J. Earth Sci.*, *34*, 1156–1166.

Cahill, T., and B. L. Isacks (1992), Seismicity and shape of the subducted Nazca Plate, *J. Geophys. Res.*, *97*, 17,503–17,529.

Cermak, V. (1993), Lithosphere thermal regimes in Europe, *Phys. Earth Planet. Inter.*, *79*, 179–193.

Cermak, V., and L. Rybach (Eds.) (1979), *Terrestrial Heat Flow in Europe*, 328 pp., Springer, New York.

Chapman, D. S. (1986), Thermal gradients in the continental crust, in *The Nature of the Lower Continental Crust*, edited by J. B. Dawson et al., *Geol. Soc. Spec. Publ., Geol. Soc. Am.*, *24*, 63–70.

Chapman, D. S., and H. N. Pollack (1975), Global heat flow: A new look, *Earth Planet. Sci. Lett.*, *28*, 23–32.

Christensen, N. I. (1979), Compressional wave velocities in rocks at high temperature and pressures, critical thermal gradients, and crustal low velocity layers, *J. Geophys. Res.*, *84*, 6849–6857.

Christensen, N. I., and W. D. Mooney (1995), Seismic velocity structure and composition of the continental crust: A global view, *J. Geophys. Res.*, *100*, 9761–9788.

Clauser, C., and E. Huenges (1995), Thermal conductivity of rocks and minerals, in *Rock Physics and Phase Relations: A Handbook of Physical Constants*, *Ref. Shelf Ser.*, vol. 3, edited by T. Ahrens, pp. 105–126, AGU, Washington, D. C.

Clowes, R. M., C. A. Zelt, J. R. Amor, and R. M. Ellis (1995), Lithospheric structure in the southern Canadian Cordillera from a network of seismic refraction lines, *Can. J. Earth Sci.*, *32*, 1485–1513.

Clowes, R. M., P. T. C. Hammer, G. F. Viejo, and J. K. Welford (2005), Lithospheric structure in northwestern Canada from LITHOPROBE seismic refraction and related studies: A synthesis, *Can. J. Earth Sci.*, *42*, 1277–1293.

Cooper, A. K., M. S. Marlow, D. W. Scholl, and A. J. Stevenson (1992), Evidence for Cenozoic crustal extension in the Bering Sea region, *Tectonics*, *11*, 719–731.

Cull, J. (1991), Heat flow and regional geophysics in Australia, in *Terrestrial Heat Flow and the Lithosphere Structure*, edited by V. Cermak and L. Rybach, pp. 486–500, Springer, New York.

Currie, C. A. (2004), The thermal structure of subduction zones and backarcs, Ph.D. thesis, 267 pp., Univ. of Victoria, Victoria, B. C., Canada.

Currie, C. A., K. Wang, R. D. Hyndman, and J. He (2004), The thermal effects of steady-state slab-driven mantle flow above a subducting plate: The Cascadia subduction zone and backarc, *Earth Planet. Sci. Lett.*, *223*, 35–48.

Davis, E. E., and T. J. Lewis (1984), Heat flow in a backarc environment: Intermontane and Omineca Crystalline belts, southern Canadian Cordillera, *Can. J. Earth Sci.*, *21*, 715–726.

Defant, M. J., and M. S. Drummond (1990), Derivation of some modern arc magmas by melting of young subducted lithosphere, *Nature*, *347*, 662–665.

Dixon, J. E., T. H. Dixon, D. R. Bell, and R. Malservisi (2004), Lateral variation in upper mantle viscosity: Role of water, *Earth Planet. Sci. Lett.*, *222*, 451–467.

Ellis, S., C. Beaumont, R. Jamieson, and G. Quinlan (1998), Continental collision including a weak zone—The vise model and its application to the Newfoundland Appalachians, *Can. J. Earth Sci.*, *35*, 1323–1346.

Engebretson, D. C., A. Cox, and R. G. Gordon (1985), Relative motions between oceanic and continental plates in the Pacific basin, *Spec. Pap. Geol. Soc. Am.*, *206*, 59 pp.

Epp, D., P. J. Grim, and M. G. Langseth (1970), Heat flow in the Caribbean and Gulf of Mexico, *J. Geophys. Res.*, *75*, 5655–5669.

Estabrook, C. H., D. B. Stone, and J. N. Davies (1988), Seismotectonics of northern Alaska, *J. Geophys. Res.*, *93*, 12,026–12,040.

Flanagan, M. P., and D. A. Wiens (1994), Radial upper mantle attenuation structure of inactive back arc basins from differential shear wave measurements, *J. Geophys. Res.*, *99*, 15,469–15,485.

Fliedner, M. M., and S. L. Klemperer (2000), Crustal structure transition from oceanic arc to continental arc, eastern Aleutian Islands and Alaska Peninsula, *Earth Planet. Sci. Lett.*, *179*, 567–579.

Flück, P. (2003), Contributions to the geodynamics of western Canada, Ph.D. thesis, 326 pp., Univ. of Victoria, Victoria, B. C., Canada.

Flück, P., R. D. Hyndman, and C. Lowe (2003), Effective elastic thickness T_e of the lithosphere in western Canada, *J. Geophys. Res.*, *108*(B9), 2430, doi:10.1029/2002JB002201.

Forsyth, D. W., and Y. Yang (2005), Small-scale convection and anisotropy in the mantle beneath southern California from high-resolution Rayleigh wave tomography, *Eos Trans. AGU*, *86*(52), Fall Meet. Suppl., Abstract T21D-06.

Frederiksen, A. W., M. G. Bostock, J. C. Van Decar, and J. F. Cassidy (1998), Seismic structure of the upper mantle beneath the northern Canadian Cordillera from teleseismic travel-time inversion, *Tectonophysics*, *294*, 43–55.

Frederiksen, A. W., M. G. Bostock, and J. F. Cassidy (2001), S-wave velocity structure of the Canadian upper mantle, *Phys. Earth Planet. Inter.*, *124*, 175–191.

Gabrielse, H. (1992), Structural styles, in *The Geology of North America*, vol. G-2, *Geology of the Cordilleran Orogen in Canada*, edited by H. Gabrielse and C. J. Yorath, pp. 571–675, Geol. Soc. of Am., Boulder, Colo.

Gaina, C., D. R. Muller, J.-Y. Royer, J. Stock, J. Hardebeck, and P. Symonds (1998), The tectonic history of the Tasman Sea: A puzzle of 13 pieces, *J. Geophys. Res.*, *103*, 12,413–12,433.

Gao, W., S. P. Grand, W. S. Baldridge, D. Wilson, M. West, J. F. Ni, and R. Aster (2004), Upper mantle convection beneath the central Rio Grande rift imaged by P and S wave tomography, *J. Geophys. Res.*, *109*, B03305, doi:10.1029/2003JB002743.

Gasparon, M., and R. Varne (1995), Sumatran granitoids and their relationship to Southeast Asian terranes, *Tectonophysics*, *251*, 277–299.

Gill, J. (1981), *Orogenic Andesites and Plate Tectonics*, 390 pp., Springer, New York.

Goes, S., and S. van der Lee (2002), Thermal structure of the North American uppermost mantle inferred from seismic tomography, *J. Geophys. Res.*, *107*(B3), 2050, doi:10.1029/2000JB000049.

Goes, S., R. Govers, and P. Vacher (2000), Shallow mantle temperatures under Europe from P and S wave tomography, *J. Geophys. Res.*, *105*, 11,153–11,169.

Goes, S., F. J. Simons, and K. Yoshizawa (2005), Seismic constraints on temperature of the Australian uppermost mantle, *Earth Planet. Sci. Lett.*, *236*, 227–237.

Gomberg, J. S., K. F. Priestly, T. G. Masters, and J. N. Brune (1988), The structure of the crust and upper mantle of northern Mexico, *Geophys. J.*, *94*, 1–20.

Gorbatov, A., J. Dominguez, G. Suarez, V. Kostoglodov, D. Zhao, and E. Gordeev (1999), Tomographic imaging of the P-wave velocity structure beneath the Kamchatka peninsula, *Geophys. J. Int.*, *137*, 269–279.

Gough, D. I. (1986), Mantle upflow tectonics in the Canadian Cordillera, *J. Geophys. Res.*, *91*, 1909–1919.

Grand, S. P. (1994), Mantle shear structure beneath the Americas and surrounding oceans, *J. Geophys. Res.*, *99*, 11,591–11,621.

Haberland, C., and A. Rietbrock (2001), Attenuation tomography in the western central Andes: A detailed insight into the structure of a magmatic arc, *J. Geophys. Res.*, *106*, 11,151–11,167.

Hall, R., and C. K. Morley (2004), Sundland basins, in *Continent-Ocean Interactions within East Asian Marginal Seas*, *Geophys. Monogr. Ser.*, vol. 149, edited by P. Clift et al., pp. 55–85, AGU, Washington, D. C.

Hall, R., and G. Nichols (2002), Cenozoic sedimentation and tectonics in Borneo: Climatic influences on orogenesis, in *Sediment Flux to Basins: Causes, Controls and Consequences*, edited by S. J. Jones and L. Frostick, *Geol. Soc. Spec. Publ.*, *191*, 5–22.

Hamilton, W. (1979), Tectonics of the Indonesian region, *U.S. Geol. Surv. Prof. Pap.*, *1078*, 345 pp.

Hamza, V. M., and M. Munoz (1996), Heat flow map of South America, *Geothermics*, *25*, 599–646.

Harder, M., and J. K. Russell (2006), Thermal state of the upper mantle beneath the Northern Cordilleran Volcanic Province (NCVP), British Columbia, Canada, *Lithos*, *87*, 1–22.

Hatcher, R. D., Jr. (1989), Tectonic synthesis of the U.S. Appalachians, in *The Geology of North America*, vol. F-2, *The Appalachian-Ouachit Orogen in the United States*, edited by R. D. Hatcher Jr., W. A. Thomas, and G. W. Viele, pp. 511–535, Geol. Soc. of Am., Boulder, Colo.

Hirth, G., and D. L. Kohlstedt (1996), Water in the oceanic upper mantle: Implications for rheology, melt extraction and the evolution of the lithosphere, *Earth Planet. Sci. Lett.*, *144*, 93–108.

Hoke, L., D. R. Hilton, S. H. Lamb, K. Hammerschmidt, and H. Friedrichsen (1994), ^{3}He evidence for a wide zone of active mantle melting beneath the central Andes, *Earth Planet. Sci. Lett.*, *128*, 341–355.

Honda, S., and M. Saito (2003), Small-scale convection under the backarc occurring in the low viscosity wedge, *Earth Planet. Sci. Lett.*, *216*, 703–715.

Honda, S., and T. Yoshida (2005), Application of the model of small-scale convection under the island arc to the NE Honshu subduction zone, *Geochem. Geophys. Geosyst.*, *6*, Q01002, doi:10.1029/2004GC000785.

Honda, S., M. Saito, and T. Nakakuki (2002), Possible existence of small-scale convection under the backarc, *Geophys. Res. Lett.*, *29*(21), 2043, doi:10.1029/2002GL015853.

Hyndman, R. D., and T. J. Lewis (1999), Geophysical consequences of the Cordillera-Craton thermal transition in southwestern Canada, *Tectonophysics*, *306*, 397–422.

Hyndman, R. D., and S. M. Peacock (2003), Serpentinization of the forearc mantle, *Earth Planet. Sci. Lett.*, *212*, 417–432.

Hyndman, R. D., C. A. Currie, and S. Mazzotti (2005), Subduction zone backarcs, continental mobile belts, and orogenic heat, *GSA Today*, *15*(2), 4–10.

Ida, Y. (1983), Convection in the mantle wedge above the slab and tectonic processes in subduction zones, *J. Geophys. Res.*, *88*, 7449–7456.

Ivins, E. R., and T. S. James (1999), Simple models for late Holocene and present-day Patagonian glacier fluctuations and predications of a geodetically detectable isostatic response, *Geophys. J. Int.*, *138*, 601–624.

James, T. S., J. J. Clague, K. Wang, and I. Hutchinson (2000), Postglacial rebound at the northern Cascadia subduction zone, *Quat. Sci. Rev.*, *19*, 1527–1541.

Jarvis, G. T., and D. P. McKenzie (1980), Sedimentary basin formation with finite extension rates, *Earth Planet. Sci. Lett.*, *48*, 42–52.

Jaupart, C., and J. C. Mareschal (1999), The thermal structure and thickness of continental roots, *Lithos*, *48*, 93–114.

Jaupart, C., J. R. Mann, and G. Simmons (1982), A detailed study of the distribution of heat flow and radioactivity in New Hampshire (U.S.A.), *Earth Planet. Sci. Lett.*, *59*, 267–287.

Jaupart, C., J. C. Mareschal, L. Guillou-Frottier, and A. Davaille (1998), Heat flow and thickness of the lithosphere in the Canadian Shield, *J. Geophys. Res.*, *103*, 15,269–15,289.

Jin, D. J., and E. Herrin (1980), Surface wave studies of the Bering Sea and Alaska area, *Bull. Seismol. Soc. Am.*, *70*, 2117–2144.

Johnston, S. T., and D. J. Thorkelson (1997), Cocos-Nazca slab window beneath Central America, *Earth Planet. Sci. Lett.*, *146*, 465–474.

Jolivet, L., K. Tamaki, and M. Fournier (1994), Japan Sea, opening history and mechanism: A synthesis, *J. Geophys. Res.*, *99*, 22,237–22,259.

Jordan, T. H. (1978), Composition and development of continental lithosphere, *Nature*, *274*, 544–548.

Kaila, K. L., and V. G. Krishna (1984), Upper mantle velocity structure in the Kurile Islands, Kamchatka, and the Sea of Okhotsk regions, *Bull. Seismol. Soc. Am.*, *74*, 2269–2296.

Karato, S. (1993), Importance of anelasticity in the interpretation of seismic tomography, *Geophys. Res. Lett.*, *20*, 1623–1626.

Karig, D. E. (1971), Origin and development of marginal basins in the western Pacific, *J. Geophys. Res.*, *76*, 2542–2561.

Kelemen, P. B., J. L. Rilling, E. M. Parmentier, L. Mehl, and B. R. Hacker (2003), Thermal structure due to solid-state flow in the mantle wedge beneath arcs, in *Inside the Subduction Factory*, *Geophys. Monogr. Ser.*, vol. 138, edited by J. Eiler, pp. 293–311, AGU, Washington, D. C.

Keller, G. R., and R. D. Hatcher Jr. (1999), Some comparisons of the structure and evolution of the southern Appalachian-Ouachita orogen and portions of the Trans-European Suture Zone region, *Tectonophysics*, *314*, 43–68.

Kennett, B. L. N., E. R. Engdahl, and R. Buland (1995), Constraints on seismic velocities in the Earth from traveltimes, *Geophys. J. Int.*, *122*, 108–124.

Klotz, J., G. Khazaradze, D. Angermann, C. Reiger, R. Perdomo, and O. Cifuentes (2001), Earthquake cycle dominates the contemporary crustal deformation in central and southern Andes, *Earth Planet. Sci. Lett.*, *193*, 437–446.

Kogan, M. G. (1975), Gravity field of the Kuril-Kamchatka Arc and its relation to the thermal regime of the lithosphere, *J. Geophys. Res.*, *80*, 1381–1390.

Konstantinovskaia, E. A. (2001), Arc-continent collision and subduction reversal in the Cenozoic evolution of the northwest Pacific: An example from Kamchatka (NE Russia), *Tectonophysics*, *333*, 75–94.

Langseth, M. G., M. A. Hobart, and K. Horai (1980), Heat flow in the Bering Sea, *J. Geophys. Res.*, *85*, 3740–3750.

Lebedev, S., and G. Nolet (2003), Upper mantle beneath Southeast Asia from S velocity tomography, *J. Geophys. Res.*, *108*(B1), 2048, doi:10.1029/2000JB000073.

Ledo, J., and A. G. Jones (2005), Temperature of the upper mantle beneath the Intermontane Belt, northern Canadian Cordillera, determined from combining mineral compositions, electrical conductivity laboratory studies and magnetotelluric field observations, *Earth Planet. Sci. Lett.*, *236*, 258–268.

Lee, T., and L. A. Lawver (1995), Cenozoic plate reconstruction of Southeast Asia, *Tectonophysics*, *251*, 85–138.

Levshin, A. L., M. H. Ritzwoller, M. P. Barmin, A. Villasenor, and C. A. Padgett (2001), New constraints on the Arctic crust and uppermost mantle: Surface wave group velocities, P_n and S_n, *Phys. Earth Planet. Inter.*, *123*, 185–204.

Lewis, T. J., W. H. Bentkowski, E. E. Davis, R. D. Hyndman, J. G. Souther, and J. A. Wright (1988), Subduction of the Juan de Fuca Plate: Thermal consequences, *J. Geophys. Res.*, *93*, 15,207–15,225.

Lewis, T. J., W. H. Bentkowski, and R. D. Hyndman (1992), Crustal temperatures near the Lithoprobe Southern Canadian Cordillera transect, *Can. J. Earth Sci.*, *29*, 1197–1214.

Lewis, T. J., R. D. Hyndman, and P. Flück (2003), Heat flow, heat generation, and crustal temperatures in the northern Canadian Cordillera: Thermal control of tectonics, *J. Geophys. Res.*, *108*(B6), 2316, doi:10.1029/2002JB002090.

Liu, M., and K. P. Furlong (1993), Crustal shortening and Eocene extension in the southeastern Canadian Cordillera: Some thermal and rheological considerations, *Tectonics*, *12*, 776–786.

Lowe, C., and G. Ranalli (1993), Density, temperature, and rheological models for the southeastern Canadian Cordillera: Implications for its geodynamic evolution, *Can. J. Earth Sci.*, *30*, 77–93.

Lowry, A. R., and R. B. Smith (1994), Flexural rigidity of the Basin and Range–Colorado Plateau–Rocky Mountain transition from coherence analysis of gravity and topography, *J. Geophys. Res.*, *99*, 20,123–20,140.

Lowry, A. R., and R. B. Smith (1995), Strength and rheology of the western U.S. Cordillera, *J. Geophys. Res.*, *100*, 17,947–17,963.

Lucassen, F., S. Lewerenz, G. Franz, J. Viramonte, and K. Mezger (1999), Metamorphism, isotopic ages and composition of lower crustal granulite xenoliths from the Cretaceous Salta Rift, Argentina, *Contrib. Mineral. Petrol.*, *134*, 325–341.

Lucassen, F. L., R. Becchio, R. Harmon, S. Kasemann, G. Franz, R. Trumbull, H.-G. Wilke, R. L. Romer, and P. Dulski (2001), Composition and density model of the continental crust at an active continental margin—The central Andes between 20° and 27°S, *Tectonophysics*, *341*, 195–223.

MacKenzie, J. M., and D. Canil (1999), Composition and thermal evolution of cratonic mantle beneath the central Archean Slave Province, NWT, Canada, *Contrib. Mineral. Petrol.*, *134*, 313–324.

Mareschal, J. C., and C. Jaupart (2004), Variations of surface heat flow and lithospheric thermal structure beneath the North American craton, *Earth Planet. Sci. Lett.*, *223*, 65–77.

McKenzie, D. P. (1969), Speculations on the consequences and causes of plate motions, *Geophys. J. R. Astron. Soc.*, *18*, 1–32.

McKenzie, D. P., and J. G. Sclater (1968), Heat flow inside the island arcs of the Northwestern Pacific, *J. Geophys. Res.*, *73*, 3173–3179.

McNamara, D. E., and M. E. Pasyanos (2002), Seismological evidence for a sub-volcanic arc mantle wedge beneath the Denali volcanic gap, Alaska, *Geophys. Res. Lett.*, *29*(16), 1814, doi:10.1029/2001GL014088.

Meschede, M., and W. Frisch (1998), A plate-tectonic model for the Mesozoic and Early Cenozoic history of the Caribbean plate, *Tectonophysics*, *296*, 269–291.

Monger, J. W. H., and R. A. Price (2002), The Canadian Cordillera: Geology and tectonic evolution, *CSEG Rec. February 2002*, pp. 17–36, Can. Soc. of Explor. Geophys., Calgary, Alberta.

Mooney, W. D., G. Laske, and T. G. Masters (1998), CRUST 5.1: A global crustal model at 5° × 5°, *J. Geophys. Res.*, *103*, 727–748.

Morgan, P. (1983), Constraints on rift thermal processes from heat flow and uplift, *Tectonophysics*, *94*, 277–298.

Nakajima, J., and A. Hasegawa (2003), Estimation of thermal structure in the mantle wedge of northeastern Japan from seismic attenuation data, *Geophys. Res. Lett.*, *30*(14), 1760, doi:10.1029/2003GL017185.

Nyblade, A. A., and H. N. Pollack (1993), A comparative study of parameterized and full thermal-convection models in the interpretation of heat flow from cratons and mobile belts, *Geophys. J. Int.*, *113*, 747–751.

Okuno, J., and M. Nakada (1998), Rheological structure of the upper mantle inferred from the Holocene sea-level change along the west coast of Kyushu, Japan, in *Dynamics of the Ice Age Earth: A Modern Perspective, GeoResearch Forum Series*, edited by P. Wu, pp. 443–458, Trans Tech, Zurich.

Oncken, O., et al. (2003), Seismic imaging of a convergent continental margin and plateau in the central Andes (Andean Continental Research Project 1996 (ANCORP'96)), *J. Geophys. Res.*, *108*(B7), 2328, doi:10.1029/2002JB001771.

O'Reilly, S. Y., W. L. Griffin, and O. Gaul (1997), Paleogeothermal gradients in Australia: Key to 4–D lithosphere mapping, *J. Aust. Geol. Geophys.*, *17*, 63–72.

Oxburgh, E. R., and D. L. Turcotte (1968), Problem of high heat flow and volcanism associated with zones of descending mantle convective flow, *Nature*, *218*, 1041–1043.

Pavlenkova, N. I. (1996), Crust and upper mantle structure in northern Eurasia from seismic data, *Adv. Geophys.*, *37*, 1–133.

Peacock, S. M. (1993), Large-scale hydration of the lithosphere above subducting slabs, *Chem. Geol.*, *108*, 49–59.

Peacock, S. M. (1996), Thermal and petrologic structure of subduction zones, in *Subduction: Top to Bottom*, *Geophys. Monogr. Ser.*, vol. 96, edited by G. E. Bebout et al., pp. 119–133, AGU, Washington, D. C.

Peacock, S. M. (2003), Thermal structure and metamorphic evolution of subducting slabs, in *Inside the Subduction Factory*, *Geophys. Monogr. Ser.*, vol. 138, edited by J. Eiler, pp. 7–22, AGU, Washington, D. C.

Perry, H. K. C., D. W. S. Eaton, and A. M. Forte (2002), LITH5.0: A revised crustal model for Canada based on Lithoprobe results, *Geophys. J. Int.*, *150*, 285–294.

Pollack, H. N., S. J. Hurter, and J. R. Johnson (1993), Heat flow from the Earth's interior: Analysis of the global data set, *Rev. Geophys.*, *31*, 267–280.

Puspito, N. T., and K. Shimazaki (1995), Mantle structure and seismotectonics of the Sunda and Banda arcs, *Tectonophysics*, *251*, 215–228.

Ritzwoller, M. H., and A. L. Levshin (1998), Eurasian surface wave tomography: Group velocities, *J. Geophys. Res.*, *103*, 4839–4878.

Ritzwoller, M. H., M. P. Barmin, A. Villasenor, A. L. Levshin, and E. R. Engdahl (2002), P_n and S_n tomography across Eurasia to improve regional seismic event locations, *Tectonophysics*, *358*, 39–55.

Robertson Maurice, S. D., D. A. Wiens, K. D. Koper, and E. Vera (2003), Crustal and upper mantle structure of southernmost South America inferred from regional waveform inversion, *J. Geophys. Res.*, *108*(B1), 2038, doi:10.1029/2002JB001828.

Rosas-Elguera, J., L. Ferrari, V. H. Garduno-Monroy, and J. Urrutia-Fucugauchi (1996), Continental boundaries of the Jalisco block and their influence in the Pliocene-Quarternary kinematics of western Mexico, *Geology*, *24*, 921–924.

Ross, J. V. (1983), The nature and rheology of the Cordilleran upper mantle of British Columbia: Inferences from peridotite xenoliths, *Tectonophysics*, *100*, 321–357.

Roy, R. F., D. D. Blackwell, and E. R. Decker (1972), Continental heat flow, in *The Nature of the Solid Earth*, edited by E. C. Robertson, pp. 506–543, McGraw-Hill, New York.

Rudnick, R. L., and D. M. Fountain (1995), Nature and composition of the continental crust: A lower crustal perspective, *Rev. Geophys.*, *33*, 267–309.

Rudnick, R. L., W. F. McDonough, and R. J. O'Connell (1998), Thermal structure, thickness and composition of continental lithosphere, *Chem. Geol.*, *145*, 395–411.

Russell, J. K., and M. G. Kopylova (1999), A steady state conductive geotherm for the north central Slave, Canada: Inversion of petrological data from the Jericho Kimberlite pipe, *J. Geophys. Res.*, *104*, 7089–7101.

Sadeghi, H., S. Suzuki, and H. Takenaka (2000), Tomographic low-velocity anomalies in the uppermost mantle around the northeastern edge of Okinawa trough, the backarc of Kyushu, *Geophys. Res. Lett.*, *27*, 277–280.

Saruwatari, K., S. Ji, C. Long, and M. H. Salisbury (2001), Seismic anisotropy of mantle xenoliths and constraints on upper mantle structure beneath the southern Canadian Cordillera, *Tectonophysics*, *339*, 403–426.

Sass, J. H., A. H. Lachenbruch, R. H. Moses Jr., and P. Morgan (1992), Heat flow from a scientific research well at Cajon Pass, California, *J. Geophys. Res.*, *97*, 5017–5030.

Schmitz, M., W.-D. Heinsohn, and F. R. Schilling (1997), Seismic, gravity and petrological evidence for partial melt beneath the thickened central Andean crust (21–23°S), *Tectonophysics*, *270*, 313–326.

Schurr, B., G. Asch, A. Rietbrock, R. Trumbull, and C. Haberland (2003), Complex patterns of fluid and melt transport in the central Andean subduction zone revealed by attenuation tomography, *Earth Planet. Sci. Lett.*, *205*, 105–119.

Sclater, J. G. (1972), Heat flow and elevation of the marginal basins of the western Pacific, *J. Geophys. Res.*, *77*, 5705–5719.

Seno, T., T. Sakurai, and S. Stein (1996), Can the Okhotsk Plate be discriminated from the North American Plate?, *J. Geophys. Res.*, *101*, 11,305–11,315.

Shapiro, N. M., and M. H. Ritzwoller (2004), Thermodynamic constraints on seismic inversions, *Geophys. J. Int.*, *157*, 1175–1188.

Shapiro, N. M., A. V. Gorbatov, E. Gordeev, and J. Dominguez (2000), Average shear-wave velocity structure of the Kamchatka peninsula from dispersion of surface waves, *Earth Planets Space*, *52*, 573–577.

Simons, F. J., A. Zielhuis, and R. D. van der Hilst (1999), The deep structure of the Australian continent from surface wave tomography, *Lithos*, *48*, 17–43.

Sleep, N., and M. N. Toksoz (1971), Evolution of marginal basins, *Nature*, *233*, 548–550.

Sobolev, S. V., H. Zeyen, G. Stoll, F. Werling, R. Altherr, and K. Fuchs (1996), Upper mantle temperatures from teleseismic tomography of French Massif Central including effects of composition, mineral reactions, anharmonicity, anelasticity and partial melt, *Earth Planet. Sci. Lett.*, *139*, 147–163.

Soyer, W., and M. Unsworth (2006), Deep electrical structure of the northern Cascadia (British Columbia, Canada) subduction zone: Implications for the distribution of fluids, *Geology*, *34*, 53–56.

Springer, M., and A. Forster (1998), Heat-flow density across the central Andean subduction zone, *Tectonophysics*, *291*, 123–139.

Stein, C. A., and S. Stein (1992), A model for the global variation in oceanic depth and heat flow with lithospheric age, *Nature*, *359*, 123–129.

Stern, C. R., F. A. Frey, K. Futa, R. E. Zartman, Z. Peng, and T. K. Kyser (1990), Trace-element and Sr, Nd, Pb, and O isotopic composition of Pliocene and Quaternary alkali basalts of the Patagonian Plateau lavas of southernmost South America, *Contrib. Mineral. Petrol.*, *104*, 294–308.

Stern, C. R., R. Kilian, B. Olker, E. H. Hauri, and T. K. Kyser (1999), Evidence from mantle xenoliths for relatively thin (<100 km) continental lithosphere below the Phanerozoic crust of southernmost South America, *Lithos*, *48*, 217–235.

Stern, R. J. (2002), Subduction zones, *Rev. Geophys.*, *40*(4), 1012, doi:10.1029/2001RG000108.

Stone, D. B., J. N. Stihler, and C. H. Estabrook (1987), Basement (P_n) velocities in Interior Alaska and the Yukon Flats, *Eos Trans. AGU*, *68*, 1458.

Sugrobov, V. M., and F. A. Yanovsky (1993), Terrestrial heat flow, estimation of deep temperature and seismicity of the Kamchatka region, *Tectonophysics*, *217*, 43–53.

Takahashi, H., et al. (1999), Velocity field of around the Sea of Okhotsk and Sea of Japan regions determined from a new continuous GPS network, *Geophys. Res. Lett.*, *26*, 2533–2536.

Tatsumi, Y., M. Sakuyama, H. Fukuyami, and I. Kushiro (1983), Generation of arc basalt magmas and thermal structure of the mantle wedge in subduction zones, *J. Geophys. Res.*, *88*, 5815–5825.

Tharmin, M. (1985), An investigation of the relationship between the geology of Indonesian sedimentary basins and heat flow density, *Tectonophysics*, *121*, 45–62.

Thompson, A. B. (1992), Water in the Earth's upper mantle, *Nature*, *358*, 295–302.

Ulmer, P. (2001), Partial melting in the mantle wedge—The role of H_2O in the genesis of mantle-derived "arc-related" magmas, *Phys. Earth Planet. Inter.*, *127*, 215–232.

Vacquier, V., S. Uyeda, M. Yasui, J. Sclater, C. Corry, and T. Watanabe (1966), Heat flow measurements in the Northwestern Pacific, *Bull. Earthquake Res. Inst. Univ. Tokyo*, *44*, 1519–1535.

van der Lee, S., and A. W. Frederiksen (2005), Surface wave tomography applied to the North American upper mantle, in *Seismic Data Analysis and Imaging With Global and Local Arrays*, *Geophys. Monogr. Ser.*, vol. 157, edited by A. Levander and G. Nolet, pp. 67–80, AGU, Washington D. C.

van der Lee, S., and G. Nolet (1997), Upper mantle S velocity structure of North America, *J. Geophys. Res.*, *102*, 22,815–22,838.

van der Lee, S., D. James, and P. Silver (2001), Upper mantle S velocity structure of central and western South America, *J. Geophys. Res.*, *106*, 30,821–30,834.

Wagner, L. S., S. Beck, and G. Zandt (2005), Upper mantle structure in the south central Chilean subduction zone (30° to 36°S), *J. Geophys. Res.*, *110*, B01308, doi:10.1029/2004JB003238.

Wang, K. (2006), Elastic and viscoelastic models of crustal deformation in subduction earthquake cycles, in *The Seismogenic Zone of Subduction Thrust Faults*, edited by T. Dixon and J. C. Moore, Columbia Univ. Press, New York, in press.

Wang, Y., and J. C. Mareschal (1999), Elastic thickness of the lithosphere in the Central Canadian Shield, *Geophys. Res. Lett.*, *26*, 3033–3035.

Watanabe, T., M. G. Langseth, and R. N. Anderson (1977), Heat flow in back-arc basins of the western Pacific, in *Island Arcs, Deep Sea Trenches and Back-Arc Basins*, *Maurice Ewing Ser.*, vol. 1, edited by M. Talwani and W. C. Pittman III, pp. 137–161, AGU, Washington, D. C.

Wdowinski, S., and Y. Bock (1994), The evolution of deformation and topography of high elevated plateaus: 2. Application to the central Andes, *J. Geophys. Res.*, *99*, 7121–7130.

Wheeler, J. O., and P. McFeely (1991), Tectonic assemblage map of the Canadian Cordillera and adjacent parts of the United States of America, *Map 1712A*, scale:1:2000000, Geol. Surv. of Can., Ottawa, Ont., Canada.

Wickens, A. J. (1977), The upper mantle of southern British Columbia, *Can. J. Earth Sci.*, *14*, 1100–1115.

Widiyantoro, S., and R. van der Hilst (1997), Mantle structure beneath Indonesia inferred from high-resolution tomographic imaging, *Geophys. J. Int.*, *130*, 167–182.

Wiens, D. A., and G. P. Smith (2003), Seismological constraints on structure and flow patterns within the mantle wedge, in *Inside the Subduction Factory*, *Geophys. Monogr. Ser.*, vol. 138, edited by J. Eiler, pp. 59–81, AGU, Washington, D. C.

Yamano, M. (1995), Recent heat flow studies in and around Japan, in *Terrestrial Heat Flow and Geothermal Energy in Asia*, edited by M. L. Gupta and M. Yamano, pp. 173–201, IBH, Bombay, India.

Yuan, X., S. V. Sobolev, and R. Kind (2002), Moho topography in the central Andes and its geodynamic implications, *Earth Planet. Sci. Lett.*, *199*, 389–402.

Zelt, C. A., and D. J. White (1995), Crustal structure and tectonics of the southeastern Canadian Cordillera, *J. Geophys. Res.*, *100*, 24,255–24,273.

Zhang, Y.-S., and R. Tanimoto (1993), High-resolution global upper mantle structure and plate tectonics, *J. Geophys. Res.*, *98*, 9793–9823.

Zhao, D. (2001), Seismological structure of subduction zones and its implications for arc magmatism and dynamics, *Phys. Earth Planet. Inter.*, *127*, 197–214.

Zhao, D., D. Christensen, and H. Pulpan (1995), Tomographic imaging of the Alaska subduction zone, *J. Geophys. Res.*, *100*, 6487–6504.

Ziagos, J. P., D. D. Blackwell, and F. Mooser (1985), Heat flow in southern Mexico and the thermal effects of subduction, *J. Geophys. Res.*, *90*, 5410–5420.

C. A. Currie, Department of Oceanography, Dalhousie University, Halifax, NS, Canada B3H 4J1. (claire.currie@dal.ca)

R. D. Hyndman, Pacific Geoscience Centre, Geological Survey of Canada, 9860 W Saanich Road, P.O. Box 6000, Sidney, BC, Canada V8L 4B2. (rhyndman@nrcan.gc.ca)